

Interactive comment on “Quantification of surface water volume changes in the Mackenzie Delta using satellite multi-mission data” by Cassandra Normandin et al.

RESPONSES TO THE REVIEWERS COMMENTS

5

R.C.: Reviewer's Comment

A.R.: Author's Reponse

Referee #1

10 This manuscript quantifies temporal changes of surface water volume water storage in the Mackenzie Delta based on multispectral images and altimetry data. The authors validates (1) classification of land water surface with multispectral images, (2) water level estimates by altimetry data, and (2) surface volume estimations retrieved by both multispectral and altimetry data. The manuscript is well-written and easy to follow their methodology and results. However, I am compelled to say that the present manuscript misses to demonstrate the scientific significance to stand alone in a HESS's publication.

15 The authors fail to demonstrate its originality of the manuscript. The authors described “the originality and novelty ... (P3L7)”. However, I felt that the present manuscript just applied existing approaches proposed by Frappart et al. (2006b, 2010, 2012) for long-time period in the target area. I could not understand challenges and difficulties in the present manuscript. I understand that the authors processed a number of data carefully and correctly. However, scientific paper needs to demonstrate (1) scientific questions or challenges that present human being does not know/understand, (2) to propose how to solve the issue (i.e., hypothesis) and (3) discuss to differentiate its originality from existing studies. I suggest the authors to reconstruct the manuscript again to demonstrate its originality. The present manuscript is quite good as engineering/technical description paper, but needs originality as a scientific paper.

25 We thank Referee 1 to offer us the opportunity to improve our manuscript. In the corrected version of the manuscript, we detailed in what our methodology differs from what we published before in other large-scale basins:

30 “In the past, this approach has been applied in tropical (e.g., the Amazon (Frappart et al., 2012), Mekong (Frappart et al., 2006b)) and peri-Arctic (e.g. the Lower Ob' basin, (Frappart et al., 2010) major river basins allowing to provide direct observations of the spatio-temporal dynamics of surface water storage. Several limitations prevent them to be used over estuaries and deltas. The first is the too coarse spatial resolution of the datasets used for retrieving the flood extent that ranges from 1 km with SPOT-VGT images used in the Lower Mekong Basin to ~ 0.25° with the Global Inundation Extent from Multi-Satellite (GIEMS, Papa et al., 2010) for the Lower Ob' and the Amazon basins. The second is inherent to the datasets used in these studies. For the Mekong Basin, due to the small number of available spectral bands present in the VGT sensor, a mere threshold on NDVI was applied. For the Amazon and the Lower Ob', as GIEMS dataset is using surface temperatures from SSM/I, no valid data are available at less than 50 km from the coast. The originality and novelty of the study is the use of multi-space mission

data at medium spatial, temporal and spectral resolutions to monitor surface water storage changes in a deltaic environment over a fifteen-year time period.”

We also explained which scientific questions motivated our study:

“Earlier studies pointed out i) the lack of continuous information in the Mackenzie delta to study the spatial distribution of water levels during the flood events and to analyze the relationship between flood severity and the timing and duration of break-up in the delta (Goulding et al, 2009b), ii) the importance of the tributaries to the Mackenzie River (i.e., Peel and Arctic Red rivers) on break-up and ice-jam flooding in the delta (Goulding et al., 2009a). As the goal of this study is to characterize the spatio-temporal dynamics of surface water, both in surface and storage, in the Mackenzie delta, north west territories of Canada, in response to spring ice break-up and snow melt, over the period 2000-2015, it will provide important new information for a better understanding of the hydro-climatology of the region.”

We widely modified the structure of the manuscript to put the stress on the scientific results. We added a supplementary information file for the technical aspects. We strengthened the introduction and conclusion on the interest of our study for the hydro-climatological community. We divided in the former version section 5 (results and discussion) in 2 separated sections: the results (section 5) and the discussion (section 6). You will find our detailed answers to your comments below.

[Other Issues]

RC 1: page 2 line 32: What are traditional methods?

A.R 1: We meant networks of in-situ gauge stations that are insufficiently dense in this region for the monitoring of the wetlands hydrodynamics although denser than in many regions of the world thanks to the efforts of the Canada Water Office to provide a good monitoring of Canadian rivers and lakes. We replaced this sentence with:

“However, it is nearly impossible to provide a long-term monitoring with traditional methods using in-situ measurements in such a large and heterogeneous environment. Satellite remote sensing methods are the only way to solve this problem offers a unique opportunity for the continuous observation of wetlands and floodplains”.

RC 2: page 7 – line 1-7 (Section 4.1): How did authors decide the criteria?

A.R 2: We applied the approach proposed by Sakamoto et al., (2007). In this method, as explained in our manuscript, pixels are considered as water-related pixels if:

- CASE 1: $EVI-LSWI \leq 0.05$ and $EVI < 0.3$
- CASE 2: $EVI \leq 0.05$ and $LSWI \leq 0$

In our study, for the case 2, we only use $EVI \leq 0.05$ since no negative values were found for images (Figure S1).

This approach was validated through comparison against the few available Landsat 8 images over our study area.

RC 3: page 9 – line 1: Please describe the definition of the “errors”.

A.R 3: We better defined the errors in the manuscript. For the figure 3a, surface extent is calculated using Sakamoto et al., (2007) classification: 0 = vegetation, 1 = permanent water, 2 = inundated pixel and 3 = mixed pixel. Only classes 1 and 2 are used for the figure 5a. Errors are calculated using the mixed pixels, corresponding to the class 3. This explanation has been added in the manuscript as follow:

“Following Sakamoto et al. (2007) method, all pixels of 8-day image have been classified into 4 classes: class 0 corresponding to vegetation, class 1 to permanent water, class 2 to inundation and class 3 to mixture of land and water. Map of annual average of land water surface, composed of inundated and permanent water bodies, was obtained at spatial and temporal resolutions of 500 m and 8 days respectively from June to September over the 2000-2015 period (Figure 3a) using classes 1 and 2.”

...

“Maps of errors made on land water surface duration with associated standard deviation are shown in Figure 3c and 3d over 2000-2015. Errors on land water surface duration are calculated using mixed pixels, corresponding to the class 3 in Sakamoto et al., (2007) classification. Standard deviation of error is presented in Figure 3d.”

RC 4: page 9 line 35: It is better to explain the method of Emmerton et al. (2007) since the authors used Emmerton et al.’s results for the validation.

A.R 4: The following sentence has been added to the manuscript:

Emmerton et al., (2007) classified the Mackenzie Delta habitat in lakes, channels, wetlands and dry floodplains using information from a topographic maps derived from aerial photographs taken during the 1950’s for low water periods.

RC 5: I recommend the authors to discuss generality of their approach. Namely, what kinds of difficulty do you expect if the other researchers would apply the same method for other areas?

A.R 5: In our opinion, this approach can be applied in any other deltaic and estuarine environments as MODIS and altimetry data are available globally.

We added the following sentence in the conclusion:

“This approach can be applied to any other deltaic and estuarine environments as MODIS and altimetry data are available globally. The major limitations are i) the presence of clouds and dense vegetation cover that prevent the use of MODIS images, ii) the relatively coarse spatial resolution of MODIS images, iii) the coarse coverage of altimetry tracks. They can be overcome i) using SAR images for flood extent monitoring as Frappart et al. (2005), ii) using images with a higher spatial resolution, iii) combining information the different altimetry missions orbiting simultaneously. The recent launches of Sentinel-1, Sentinel-2 and 3 offer new opportunities for flood extent monitoring at higher spatial (from ~10 m to 300 m) and temporal (a few days) resolutions”.

Referee #2

Normandin et al. used multi satellite sensor integration (multispectral and radar altimetry) to quantify both surface water extent and volume dynamics across the Mackenzie Delta for a time period of 15 years. The information (time series) generated in this study is of high relevance for many applications and the methodology used is appropriate and well documented/ described. Although this is not the first study to combine satellite altimetry with remotely sensed surface water extents for water volume estimations, the application of these methods over a large and complex river delta and a 15-year time period makes this study a significant contribution to the field and of great interest to the HESS community. Nevertheless, the manuscript is rather premature and not suitable for publication in its present form. The authors fail to clearly distinguish their work from work that has already been done and the significance and novelty of their research isn't presented in its full potential. In addition, the authors leave it up to the readers to find the key results and highlights of the research. Rather than conveying the findings in a limited number of carefully designed figures and tables, the authors present an abundance of material that makes it difficult for the reader to ingest and enjoy the paper. The writing of the paper is often in the style of a technical report and the manuscript lacks flow in the argumentation and a proper discussion section, where the limitations and implications of the research are discussed in detail. Due to these issues, the manuscript is not suitable for publication in HESS in its present form and needs to undergo major revisions before it can be considered suitable for publication.

We thank the Referee for his helpful comments that helped us in improving our manuscript. We widely modified the structure of the manuscript to put the stress on the scientific results. We added a supplementary information file for the technical aspects. We strengthened the introduction and conclusion on the interest of our study for the hydro-climatological community. We divided in the former version section 5 (results and discussion) in 2 separated sections: the results (section 5) and the discussion (section 6). You will find our detailed answers to your comments below. You will find our detailed answers to your comments below.

Specific Comments:

RC 1: The number of Figures and Tables is very high in relation to the information and novelty content of the manuscript. I highly recommend to reduce the number of Figures so that only the key information and results is presented. For example, the statistics presented in three separate tables 3,4 and 5 should be easy enough to show in a single graph, which would also make it much easier for the reader to get the main points without having to search. The same applies to the abundance of inundation extent and duration maps that are shown.

A.R 1: Following your suggestion, we reduced the number of Tables and Figures. The statistics of the validation of altimetry-based water levels were merged from three to one table. A similar merging was also applied for inundation extent. Former figures 3, 4 and 7 were moved to the supplementary information document.

RC 2: Introduction: line 7 to 23: This sounds like the study area section (which should go to methods).

A.R 2: This paragraph was merged with the existing content of the study area section (that was reduced).

5 RC 3: page 2 line 29: Thus, the understanding of these dynamic environments is a societal and scientific stake to anticipate and manage their evolutions at medium and long term time scales. This is confusing and I do not follow what your argument is here. Consider re-writing and clearly making your point.

A.R 3: We rewrote as follows:

10 “Improving our knowledge on the dynamics of the surface water reservoir in circumpolar areas is crucial for a better understanding of their role in flood hazard, carbon production, greenhouse gases emission, sediment transport, exchange of nutrients and land-atmosphere interactions”.

15 RC 4: page 2 line 33: I agree with you that they probably are the only way but I would be careful with this statement, considering that large-scale 3-d hydrodynamic modeling is getting more and more powerful and feasible. Also airborne remote sensing is an alternative. Consider rewriting.

A.R 4: To focus on the long-term monitoring, we rewrote as follows:

20 “Mapping surface water extent at the Mackenzie Delta scale is an important issue. However, it is nearly impossible to provide a long-term monitoring using in-situ measurements in such a large and heterogeneous environment. Satellite remote sensing methods offers a unique opportunity for the continuous observation of wetlands and floodplains”.

RC 5: page 3 line 4: use quantify surface water extents instead of “spatial extent of surface water extents”

A.R 5: Corrected.

25 RC 6: page 3 line 8: The whole intro is poorly structured and lacks argumentative flow, which makes it rather difficult to read. It reads a bit like a “staccato” listing of important but often slightly unrelated and repetitive pieces of information. Consider rewriting the intro with improved flow and less repetitions and focus on the a) background, b) significance and innovation and c) motivation of your research, rather than a very detailed description of your study area and
30 corresponding environmental processes. You should clearly state that the sensors that you integrated haven’t been integrated in this way for this particular quantification (if this is the case) and add more emphasis on the usefulness of the information about surface water extent and volume that you are generating in this study (which is certainly of very high importance). What can a time series of surface water volume be used for (i.e. studying climate feedback or sea level
35 rise...).

A.R 6: We completely restructured the introduction as you mentioned. We strengthened the significance and innovation (see our response to your comment below) and the motivation for this study as follows:

“Earlier studies pointed out i) the lack of continuous information in the Mackenzie delta to study the spatial distribution of water levels during the flood events and to analyze the relationship between flood severity and the timing and duration of break-up in the delta (Goulding et al, 2009b), ii) the importance of the tributaries to the Mackenzie River (i.e., Peel and Arctic Red rivers) on break-up and ice-jam flooding in the delta (Goulding et al., 2009a). As the goal of this study is to characterize the spatio-temporal dynamics of surface water, both in surface and storage, in the Mackenzie delta, north west territories of Canada, in response to spring ice break-up and snow melt, over the period 2000-2015, it will provide important new information for a better understanding of the hydro-climatology of the region”.

RC 7: page 3 line 6: Where you cite papers that have “successfully applied this approach”: You should describe the very closely related studies with more detail and then highlight what your study adds to this existing body of knowledge.

A.R 7: We added the following sentences:

“ In the past, this approach has been applied in tropical (e.g., the Amazon (Frappart et al., 2012), Mekong (Frappart et al., 2006b)) and peri-Arctic (e.g. the Lower Ob’ basin, (Frappart et al., 2010) major river basins allowing to provide direct observations of the spatio-temporal dynamics of surface water storage. Several limitations prevent them to be used over estuaries and deltas. The first is the too coarse spatial resolution of the datasets used for retrieving the flood extent that ranges from 1 km with SPOT-VGT images used in the Lower Mekong Basin to ~ 0.25° with the Global Inundation Extent from Multi-Satellite (GIEMS, Papa et al., 2010) for the Lower Ob’ and the Amazon basins. The second is inherent to the datasets used in these studies. For the Mekong Basin, due to the small number of available spectral bands present in the VGT sensor, a mere threshold on NDVI was applied. For the Amazon and the Lower Ob’, as GIEMS dataset is using surface temperatures from SSM/I, no valid data are available at less than 50 km from the coast. The originality and novelty of the study is the use of multi-space mission data at medium spatial and temporal resolutions to monitor surface water storage changes in a deltaic environment over a fifteen-year time period”.

RC 8: page 3 line 36. Given the very high relevance of existing large scale surface water extent time series for your study (you could have used some of those for validation), you may want to consider to cite the state-of-the-art literature here: Pekel, J., A. Cottam, N. Gorelick, and A. S. Belward (2016), High resolution mapping of global surface water and its long-term changes, *Nature*, 540, 418–422, doi:10.1038/nature20584. Tulbure, M. G., M. Broich, S. V Stehman, and A. Kommareddy (2016), Surface water extent dynamics from three decades of seasonally continuous Landsat time series at subcontinental scale in a semi-arid region, *Remote Sens. Environ.*, 178, 142–157, doi:10.1016/j.rse.2016.02.034. Klein, I., Gessner, U., Dietz, A.J., Kuenzer,

C., 2017. Global WaterPack – A 250 m resolution dataset revealing the daily dynamics of global inland water bodies. *Remote Sens. Environ.* 198, 345–362. doi:10.1016/j.rse.2017.06.045

A.R 8: We agree on this comment. In fact, our manuscript was ready to submit in fall 2016 when we added the comparison with Landsat-8. We added these recent references.

5

RC 9: page 3 line 10: In my opinion, the study region section is unnecessarily lengthy. Consider focusing only on the information that is relevant to your study and methods. Consider improving the reading flow by connecting sentences with similar information.

A.R 9: The section has been rewritten and is shorter taking, taking into account only important and relevant information.

10

RC 10: page 4 line 6: Are you sure it's "raw radiance"? You mention further down it's surface reflectance.

A.R 10: Corrected, it was a mistake.

RC 11: page 4 line 25: It is true that there will be plenty of data gaps in the OLI time series but what is the time step that you require for the surface water extent dynamics in your study? How quickly does the extent change over time? What about Sentinel-2?

15

A.R 11: Surface water storage dynamic happens really fast in this environment. This is why we chose to use images available every 8-day to be able to monitor the variations of surface water extent and storage. Until the launch of Landsat-8 in 2013, only 2 images were available for our study period (from June to September). Our study presents multi-year variations of surface water storage and extent. There are still too few Sentinel-2 images to allow a long-term monitoring. Besides, to our knowledge, surface reflectances from Sentinel-2 are not available in the Mackenzie, only top of atmosphere reflectances. We agree with this comment and we mentioned the interest of the Sentinel missions in the conclusion:

20

"The recent launches of Sentinel-1, Sentinel-2 and 3 offer new opportunities for flood monitoring at higher spatial (~10 m) and temporal (a few days) resolutions".

25

RC 12: page 6 line 4: You may want to consider Tulbure, Klein and Pekel 2016 and mention that the state of the art for this type of classification is machine learning but that you chose a simplified spectral indices approach because...

A.R 12: We totally agree you. Machine learning techniques need to have ground validation. This was not our case. This why we choose this approach. We added your comment to our manuscript: "As we do not have any external information to perform a supervised classification as the current state of the art machine learning techniques, we used the approach proposed by (Sakamoto et al., 2007) to monitor the land water surface extent in the Mackenzie Delta (Figure 2)".

30

35

RC 13: page 6 line 31: You think one OLI image is enough for cross-validation?

A.R 13: We used the only information available that consists of two Landsat-8 images. Two OLI images were used to validate (01/07/2013 and 02/08/2013) and validation results are shown in Table 1.

RC 14: page 7 line 8: you mean of the “annual” study period from June to September? Your study period is 2000-2015 right?

A.R 14: Yes exactly, I've added annual. Yes my study period is 2000-2015.

RC 15: page 8 line 6: What is rough delineation of cross sections? Do you have DEM data or do you just refer to location of rivers?

A.R 15: As explained in the manuscript and in the references cited, the first is a rough delineation of the cross-sections (typically plus or minus 5 km from the river banks) based on satellite images. The MAPS software allows to superimpose altimeter tracks to a Google Earth background. Then, the shape of the altimeter along-track profiles permit to identify the river that is generally materialized as a shape of “V” or “U” with the lower elevations corresponding to the water surface (see Santos da Silva et al., 2010 and Baup et al., 2014 for more details). We added this last sentence to the manuscript.

RC 16: page 8 line 9: What is the refined process?

A.R 16: We modified as follows:

“Valid altimetry data were selected through a refined process that consists in eliminating outliers and measurements over non-water surfaces based on visual inspection”.

RC 17: page12 line 24: The correlation between discharge and surface water volumes should be discussed more here. Due to the size of the delta, there would be significant lag effects (time that the flow takes to pass through the delta) that are not captured by a simple correlation. You may want to consider to have a look at similar type of models and discuss your work in that context (i.e. Heimhuber, V., Tulbure, M.G., Broich, M., 2017. Modeling multidecadal surface water inundation dynamics and key drivers on large river basin scale using multiple time series of Earth-observation and river flow data. Water Resour. Res. 53, 1–19. doi:10.1002/2016WR019858). The relationship between discharge and water volume is unlikely to be linear so an r2 of 0.66 is pretty high for your application - I recommend discussing.

A.R 17: Thank very much for your comment. As you mentioned, the situation is quite similar in the Mackenzie delta. There are some floodplains connected and some other non- connected to the river. As it is mentioned in the manuscript, after the flood peak in June, the validation performed between MODIS and Landsat showed that MODIS only detects water over river channels and connected floodplains whereas the small non-connected lakes were not. We totally agree on the non-linearity between volume and discharge. We also noted it on the first study we published using this technique (Frappart et al., 2005). We computed cross-correlations between storage and discharge. We did not found any time-lag. This lack of time-lag is likely due to the time-step of 8 days of our estimates.

We added the following paragraph in section spatio-temporal dynamics of surface water storage:

“The comparison between storage and flux (discharge) exhibits a quite good correlation ($R=0.66$ with no time-lag) between these two quantities. Several studies demonstrated that there is no linear relationship between surface water extent, surface water volume and river discharge due to the presence of floodplains non-connected to the river (e.g., Frappart et al., 2005; Heimhuber et al., 2017). Due to the small area of the non-connected lakes present in the McKenzie delta, they are detected in our approach based on the use of MODIS images at 500 m of spatial resolution, as mixture areas (except during the June flood event where almost all the delta is inundated and all the flooded areas are connected to the river). Only the floodplains connected to river are considered in this study”.

RC 18: Figure 3: A scale bar would make it easier to get an idea of the size of the index images that are shown in each panel.

A.R 18: We chose to display the geographical coordinates on each map to have both the scale and the localization. This is why, we decided not to add a scale bar.

RC 19: Figure 5: You might want to keep the direction of your colour bar consistent (i.e. more days is red, less days is blue).

A.R 19: We chose this color code to make the correspondence between blue and wetter conditions and red drier conditions. If this represents a big issue, we can modify the color bar.

RC 20: page 13 line 6 & Figure 6: Given that the surface water extent of the first time step of your annual time period is always the highest, maybe you should have started the annual time period 1 month earlier, to ensure that you always capture the peak of the flood extent. I find it problematic that you state that surface water extent is maximum in June, given that you never looked at May.

A.R 20: We did not use the images from May as in most of the cases, there are still snow and ice. We added the following sentence in the manuscript: “Images from May were not used due to the presence of remaining snow and ice in the Mackenzie delta”

RC 21 : Figure 7: How about overlaying the classified 500m pixel MODIS and Landsat image to highlight the differences. Give pixels where both agree one colour and then another colour for only water on Landsat and one for only water on MODIS.

A.R 21: Following your comment, I've done this figure and introduced it in the supplementary script (Figure S4). Yellow pixels are corresponding to water in the both images (MODIS and OLI 500), light blue to water only for OLI 500 and dark blue to water only for MODIS.

Technical Corrections:

RC 22 : page 1, line 20: In this study, the dynamics of surface water extent and volume “are or were” analyzed from 2000 to 2015 by combining multi-satellite information from MODIS multispectral images at 500 m spatial resolution and river stages derived from ERS-2 (1995-2003), ENVISAT (2002-2010) and SARAL (since 2013) altimetry data.

A.R 22: Corrected.

RC 23: page 2 Line 5: Discharge instead of discharger

A.R 23: Corrected.

RC 24: page 7 line 10: you mean Hereafter?

A.R 24: « Hereafter » and « Thereafter », have close meanings. We chose « Thereafter » meaning « from then ».

RC 25: page 13 line 11: “.” missing after MODIS?

A.R 25: Corrected.

RC 26: page 13 line 20: mistake in “Frthat”

A.R 26: Corrected.

RC 27: page 13 line 23: Sentence starting with “Besides, these...” is gramatically wrong and I do not get the point.

A.R 27: This sentence was modified as follows:

“These products provide a unique long-term dataset that allows a continuous monitoring of the changes affecting the surface water reservoir before the launch of the NASA-CNES Surface Water and Ocean Topography (SWOT) mission in 2021. The recent launches of Sentinel-1, Sentinel-2 and 3 offer new opportunities for flood monitoring at higher spatial (~10 m) and temporal (a few days) resolutions”.

Quantification of surface water volume changes in the Mackenzie Delta using satellite multi-mission data

Cassandra Normandin¹, Frédéric Frappart^{2, 3}, Bertrand Lubac¹, Simon Bélanger⁴, Vincent Marieu¹, Fabien Blarel³, Arthur Robinet¹ and Léa Guiastrennec-Faugas¹

¹ EPOC, UMR 5805, Université de Bordeaux, Allée Geoffroy Saint-Hilaire, 33615 Pessac, France

² GET-GRGS, UMR 5563, CNRS/IRD/UPS, Observatoire Midi-Pyrénées, 31400 Toulouse, France

³ LEGOS-GRGS, UMR 5566, CNRS/IRD/UPS, Observatoire Midi-Pyrénées, 31400 Toulouse, France

⁴ Dép. Biologie, Chimie et Géographie, groupe BOREAS and Québec-Océan, Université du Québec à Rimouski, 300 allée des ursulines, Rimouski, Qc, G5L 3A1, Canada

Correspondence to: Cassandra Normandin (cassandra.normandin@u-bordeaux.fr)

Abstract. Quantification of surface water storage in extensive floodplains and their dynamics are crucial for a better understanding of global hydrological and biogeochemical cycles. In this study, we present estimates of both surface water extent and storage combining multi-missions remotely-sensed observations and their temporal evolution over more than 15 years in the Mackenzie Delta. The Mackenzie Delta is located in the North West of Canada and is the second largest delta in the Arctic Ocean. The delta is frozen from October to May and the recurrent ice break up provokes an increase of the river's flows. Thus, this phenomenon causes intensive floods along the delta every year with dramatic environmental impacts. In this study, the dynamics of surface water extent and volume are analyzed from 2000 to 2015 by combining multi-satellite information from MODIS multispectral images at 500 m spatial resolution and river stages derived from ERS-2 (1995-2003), ENVISAT (2002-2010) and SARAL (since 2013) altimetry data. The surface water extent (permanent water and flooded area) peaked in June with an area of 9,600 km² (+/- 200 km²) on average, representing approximately 70% of the delta's total surface. Altimetry-based water levels exhibit annual amplitudes ranging from 4 m in the downstream part to more than 10 m in the upstream part of the Mackenzie Delta. A high overall correlation between the satellite-derived and in situ water heights ($R > 0.84$) is found for the three altimetry missions. Finally, using altimetry-based water levels and MODIS-derived surface water extents, maps of interpolated water heights over the surface water extents are produced. Results indicate a high variability of the water height magnitude that can reach 10 meters compared to the lowest water height in the upstream part of the delta during the flood peak in June. Furthermore, the total surface water volume is estimated and shows an annual variation of approximately 8.5 km³ during the whole study period, with a maximum of 14.4 km³ observed in 2006. The good agreement between the total surface water volume retrievals and in situ river discharges ($R = 0.66$) allows validating this innovative multi-mission approach and highlights the high potential to study the surface water extent dynamics.

Key words: Mackenzie Delta, surface water extent, multispectral imagery, satellite altimetry, surface water volume

1 Introduction

Monitoring the temporal and spatial variations in water stored or transiting, such as rivers, floodplain wetlands and lakes is essential (Seyler et al., 2008). Although wetlands and floodplain cover only 6% of the surface of the Earth (OECD, 1996), they are a key reservoir in hydrological and biogeochemical cycles. These areas play a major role in flood flow alteration, sediment stabilization settling, water quality, groundwater recharge and discharge (Maltby, 1990; Bullock and Acreman, 2003).

The Mackenzie Delta, a floodplain system located in Canada's western Arctic, is flat and composed of numerous lakes (Are and Reimnitz, 2000) and host large populations of birds, fishes and mammals (Beltaos, 2013; Squires et al., 2009). These lakes are ecologically sensitive environments largely controlled by river water (Squires et al., 2009). The Mackenzie Delta is ice covered during 7-8 months per year (Emmerton et al., 2007). The Mackenzie River flows northward from relatively warm area toward colder northern regions. The river ice break up starts in the South in March-April and progresses to the North to reach the delta sometime in May-June (Pavelsky and Smith, 2004). During the freshet, the freshwater meets an ice dam that was formed in winter along the shoreline of the Beaufort Sea known as the Stamukhi zone (Carmack and Macdonald, 2002) creating a large scale flooding of the delta. Ice breakup related floods can increase water levels to much higher elevations than open water floods (Beltaos and Carter, 2009). This is one of the most important annual hydrologic events in cold regions (Muhammad et al., 2016). Floods are at the origin of significant surface water storage in the delta (Holmes et al., 2012; Pithan and Mauritsen, 2014).

These important recurrent floods replenish delta lakes with river water, sediments, and nutrients and play an important role in the maintenance of their ecosystems (Beltaos et al., 2012). It generates many environmental benefits such as geochemical land deposition, groundwater recharges, but also detriments such as infrastructure damages and lost economic activities (Käab and Prowse, 2011).

Deltas are vulnerable to both anthropogenic and natural forcing such as socio-economic infrastructure development and global warming. In Arctic, the latter is particularly severe due to the polar amplification processes and complex positive feedback loops (Holmes et al., 2012). This system is undergoing important changes as the increase of precipitation at high latitudes, increase river discharge and melting of stock ices on land and sea (Stocker and Raible, 2005). These changes may induce an acceleration of the hydrologic cycle (Stocker and Raible, 2005). River discharge may increase from 18 to 70% from now to the end of the century (Peterson et al., 2002).

Improving our knowledge on the dynamics of the surface water reservoir in circumpolar areas is crucial for a better understanding of their role in flood hazard, carbon production, greenhouse gases emission, sediment transport, exchange of nutrients and land-atmosphere interactions. Thus, the understanding of these dynamic environments is a societal and scientific stake to anticipate and manage their evolutions at medium and long term time scales.

Mapping surface water extent at the Mackenzie Delta scale is an important issue. However, it is nearly impossible to provide a long-term monitoring with traditional methods with traditional methods using in-situ measurements in such a large and heterogeneous environment. Satellite remote sensing methods are the only way to solve this problem offers a unique opportunity for the continuous observation of wetlands and floodplains. Remote sensing has proven a strong potential to detect and monitor floods during the last two decades (Alsdorf et al., 2007; Smith, 1997). Typically, two kinds of sensor are used to map flooded area at high and moderate resolutions: passive multispectral imagery and active Synthetic Aperture Radar (SAR). The spectral signature of the surface reflectance

is used to discriminate between water and land (Rees, 2013~~04~~). The SAR images provide valuable information on the nature of the observed surface through the backscattering coefficient (Ulaby et al., 1981).

If space missions of radar altimetry were mainly dedicated to estimate ocean surface topography (Fu and Cazenave, 2001), it is now commonly used for monitoring inland waters levels (Birkett, 1995 ; Cazenave et al., 1997; Frappart et al., 2006a; Santos da Silva et al., 2010; Crétau et al., n.d.; Frappart et al., 2015b; [Crétau et al., 2017](#)). Several studies have shown the possibility to measure water levels variations in lakes, rivers and flooding plains (Frappart et al., 2006b, 2015a; Santos da Silva et al., 2010). In the present ~~paper~~[study](#), satellite multispectral imagery and altimetry are used in synergy to quantify ~~surface water extents~~ [the spatial extent of surface water extents](#) and the surface water volumes of the Mackenzie Delta and analyze their temporal variations. In the past, this approach has been ~~successfully~~ applied in tropical (e.g., the Amazon (Frappart et al., 2012), Mekong (Frappart et al., 2006b)) and peri-Arctic (e.g. the Lower Ob' basin, (Frappart et al., 2010) major river basins [allowing to provide direct observations of the spatio-temporal dynamics of surface water storage](#). [Several limitations prevent them to be used over estuaries and deltas.](#) The first is the too coarse spatial resolution of the datasets used for retrieving the flood extent that ranges from 1 km with SPOT-VGT images used in the Lower Mekong Basin to ~ 0.25° with the Global Inundation Extent from Multi-Satellite (GIEMS, Papa et al., 2010) for the Lower Ob' and the Amazon basins. The second is inherent to the datasets used in these studies. For the Mekong Basin, due to the ~~small~~[limited](#) number of ~~available~~ spectral bands present in the VGT sensor, a mere threshold on NDVI was applied. For the Amazon and the Lower Ob', as GIEMS dataset is using surface temperatures from SSM/I, no valid data are available at less than 50 km from the coast. ~~But,~~ The originality and novelty of the study is the use of multi-space mission data at ~~better~~[high](#) spatial, ~~and~~ temporal [and spectral](#) resolutions [than the previous studies to monitor surface water storage changes in a deltaic environment over a fifteen-year time period](#) ~~long time series allowing to improve the robustness of retrievals~~.

[Earlier studies pointed out i\) the lack of continuous information in the MeKackenzie delta to study the spatial distribution of water levels during the flood events and to analyze the relationship between flood severity and the timing and duration of break-up in the delta \(Goulding et al, 2009b; Beltaos et al., 2012\), ii\) the importance of the tributaries to the MeKackenzie River \(i.e., Peel and Arctic Red rivers\) on break-up and ice-jam flooding in the delta \(Goulding et al., 2009a\). As the goal of this study is to characterize the spatio-temporal dynamics of surface water, both in surface and storage, in the MeKackenzie delta, north west territories of Canada, in response to spring ice break-up and snow melt, over the period 2000-2015, it will provide important new information for a better understanding of the hydro-climatology of the region.](#)

2 Study region

[The Mackenzie Delta, a floodplain system, is located in the northern part of Canada \(Figure 1a\) and covers an area of 13,135 km² \(Emmerton et al., 2008\), making it the second biggest delta of Arctic with a length of 200 km and a width of 80 km \(Emmerton et al., 2008\). It is mainly drained by the Mackenzie River \(90% of the delta's water supply\) and Peel River \(8% of the delta's water supply, Emmerton et al., 2007\). The Mackenzie Delta channels have very mild slopes \(-0.02 m/km, \(Hill et al., 2001\) and is ice covered during 7-8 months per year \(Emmerton et al., 2007\).](#)

[The Mackenzie River begins in the Great Slave Lake and then, flows through the North West territories before reaching the Beaufort Sea. It has a strong seasonality in term of discharge due to \[spring ice break-up and snowmelt\]\(#\).](#)

from about 5,000 m³.s⁻¹ in winter up to 40,000 m³.s⁻¹ in June during the ice breakup for wet years (Figure 1b, Macdonald and Yu, 2006 ; Goulding et al., 2009a ; Goulding et al., 2009b ; Beltaos et al., 2012). The Stamukhi (ground accumulation of sea ice) is responsible for recurrent floods in the Mackenzie Delta. At the flood peak, 95% of the delta surface is likely to be covered with water (Macdonald and Yu, 2006). Water level peaks are mainly controlled by ice breakup effects and secondary by the amount of water contained in snowpack (Lesack and Marsh, 2010). This is one of the most important annual hydrologic events in cold regions (Muhammad et al., 2016).

The delta is a complex of multiple channels and numerous shallow and small lakes (over 49,000 lakes), covering nearly ~50% of the delta area (Emmerton et al., 2007), and are ecologically sensitive environments largely controlled by river water (Squires et al., 2009). This environment is also one of the most productive ecosystems in northern Canada with large populations of birds, fishes and mammals, which are critical resources for local population (Squires et al., 2009).

3 Data sets

3.1 Multispectral imagery

3.1.1 MODIS

The MODerate resolution Imaging Sensor (MODIS) is a spectroradiometer, part of the payload of the Aqua (since 2002) and Terra (since 1999) satellites. The MODIS sensor measures radiances in 36 spectral bands. In this study, the MOD09A1 product (8-day binned level 3, version 6) derived from Terra and Aqua-satellites raw radiance surface reflectance measurements were downloaded from the United States Geological Survey (USGS) Earthexplorer website (<http://earthexplorer.usgs.gov>). It consists in gridded, atmospherically corrected surface reflectance acquired in 7 bands from visible to short wave infrared (2155 nm) at a 500 m spatial resolution. This product is obtained combining for each wavelength the best surface reflectance data of every pixel acquired during an 8-day period. Each MODIS tile covers an area of 1200 km by 1200 km. Two tiles (h12v02 and h13v02) are used to cover the whole study area. In this study, 223 composites, acquired during the ice-free period from June to September over the 2000-2015 time-span, are used.

3.1.2 OLI

The Landsat-8 satellite is composed of two Earth-observing sensors, the Operational Land Imager (OLI) and Thermal InfraRed Sensor (TIRS). This satellite was launched in February 2013 and orbits at an altitude of 705 km. The swath is 185 km and the whole Earth surface is covered every 16 days.

The OLI/TIRS sensors measure in 11 spectral bands in the visible (450-680 nm), near infrared (845-885 nm) and short wave infrared portions (1,560-2,300 nm) of the electromagnetic spectrum. In this study, the Landsat 8/OLI surface reflectance products were downloaded from the Landsat-8 USGS portal (<http://earthexplorer.usgs.gov/>). The multispectral spatial resolution is 30 m and 15 m for panchromatic band. Two images are necessary to cover the Mackenzie Delta.

Landsat-8 mission is characterized by a lower revisit time than Terra and Aqua mission. Thus, associated with a high occurrence of clouds over the study area, Landsat-8 yields to a small amount of high-quality data. OLI images

cannot be consequently used in this study to monitor land water surface temporal changes. In this context, MODIS represent a relevant alternative to OLI despite a lower spatial resolution. However, available high-quality OLI data have been used to compare and validate MODIS land water surfaces.

3.2 Radar altimetry data

3.2.1 ERS-2

The ERS-2 satellite (European Remote Sensing) was launched in 1995 by the European Space Agency (ESA). Its payload is composed of several sensors, including a radar altimeter (RA), operating at Ku-band (13.8 GHz). It was orbiting sun-synchronously at an altitude of 790 km with an inclination of 98.54° with a 35-day repeat cycle. This orbit was ERS-1's orbit with a ground-track spacing about 85 km at the equator. ERS-2 provides observations of the topography of the Earth from 82.4° latitude north to 82.4° latitude south. ERS-2 data are disposable from 17 May 1995 to 9 August 2010 but after 22 June 2003, the coverage is limited.

3.2.2 ENVISAT

Envisat mission was launched on March 1st 2002 by ESA. This satellite carried 10 different instruments including the advanced radar altimeter (RA-2). It was based on the heritage of ERS-1 and 2 satellites. RA-2 was a nadir-looking pulse-limited radar altimeter operating at two frequencies at Ku- (13.575 GHz) and S-(3.2 GHz) bands. Its goal was to collect radar altimetry over ocean, land and ice caps (Zelli, 1999). Envisat remained on its nominal orbit until October 2010 but RA-2 stopped operating correctly at S-band in January 2008. Its initial orbital characteristics are the same as for ERS-2.

3.2.3 SARAL

SARAL mission was launched on 25 February 2013 by a partnership between CNES (Centre National d'Etudes Spatiales) and ISRO (Indian Space Research Organization). Its payload comprised the AltiKa radar altimeter and bi-frequency radiometer, and a triple system for precise orbit determination: the real-time tracking system DIODE of DORIS instrument, a Laser Retroreflector Array (LRA), and the Advance Research and Global Observation Satellite (ARGOS-3). AltiKa is the first radar altimeter to operate Ka-band (35.75 GHz). It is a solid-state mono-frequency altimeter that provides precise range estimates (Verron et al., 2015). SARAL orbit was earlier utilized by ERS-1 & 2 and ENVISAT missions with a track spacing of 85 km at the equator (Verron et al., 2015). It has been put on a drifting orbit since 4 July 2016.

Altimetry data used here are contained in the Geophysical Data Records (GDRs) and are the followings:

- cycle 001 (17/05/1995) to cycle 085 (07/08/2003) for ERS-2 from the reprocessing of the ERS-2 mission raw waveform performed at Centre de Topographie de l'Océan et de l'Hydrosphère (CTOH) (Frappart et al., 2016)
- GDR v2.1 for ENVISAT from cycle 006 (14/05/2002) to cycle 094 (21/10/2010)
- GDR E for SARAL from cycle 001 (15/03/2015) to cycle 027 (14/10/2015)

These data were made available by CTOH (<http://ctoh.legos.obs-mip.fr/>). Data were acquired along the altimeter track at 18, 20 and 40 Hz for ENVISAT, ERS -2 and SARAL respectively (high-frequency mode commonly used over land and coastal areas where the surface properties are changing more rapidly than over the open ocean).

They consist of the satellite locations and acquisition times and all the parameters necessary to compute the altimeter heights (see Section 4.3).

3.3 In situ water levels and discharges

The altimetry-based water level time-series derived from radar altimetry were compared to gauge record from in situ stations for validation purpose. Data from 10 gauge stations were found in a close vicinity of altimetry virtual stations (at a distance lower than 20 km along the streams). Virtual stations are built at intersections between an orbit groundtrack and a water body (lake, river and floodplain) (Crétaux et al., [in press 2017](#)). Besides, surface water storage variations were compared to the rivers flow entering the delta summing the records from 3 gauge stations located in upstream part of the delta. Daily data of water level and discharge were downloaded for free from the Canadian government website (<http://wateroffice.ec.gc.ca>).

4 Methods

4.1 Quantification of surface water extent

Multispectral imagery is commonly used for delineating flood extent using spectral indices (e.g., Frappart et al., 2006b; Sakamoto et al., 2007; Crétaux et al., 2011; ~~Pekel et al., 2014~~; Verpoorter et al., 2014; Ogilvie et al., 2015; Pekel et al., 2014⁶). As we do not have any external information to perform a supervised classification as the current state of the art machine learning techniques (Pekel et al., 2016; Tulbure et al., 2016; Klein et al., 2017), ~~In this study,~~ we used the approach proposed by (Sakamoto et al., 2007) to monitor the land water surface extent in the Mackenzie Delta (Figure 2). This approach is based on the application of thresholds on the Enhanced Vegetation Index (EVI), the Land Surface Water Index (LSWI) and the Difference Value between EVI and LSWI (DVEL=EVI-LSWI) to determine the status (non-flooded, ~~mixture~~^{mixed}, flooded and permanent water body) of any pixel in an 8-day MODIS composite image of surface reflectance. As the spectral response of the Near Infra-Red (NIR) and short-wave infrared (SWIR) bands are highly dependent on the Earth surface nature, in particular water versus soil/vegetation surfaces, their complementary was used to define LSWI. For instance, the surface reflectance presents low values (a few percentages) over non-turbid water bodies and high values (a few tens of percentage) over vegetation feature in the NIR spectral bands. The spectral response in the SWIR is mainly dominated by strong water absorption bands, which is directly sensitive to moisture content in the soil and the vegetation. For water surface, the signal in the SWIR is assumed to be zero even in turbid waters (Wang and Shi, 2005). Thus, LSWI is expected to get values close to 1 for water surfaces and lower values for non-water surfaces. The two indices, used in this approach, are defined as follows (Huete et al., 1997; Xiao et al., 2005):

$$EVI = a \times \frac{\rho_{NIR} - \rho_{red}}{\rho_{NIR} + b \times \rho_{red} - c \times \rho_{blue} + d} \quad (1)$$

$$LSWI = \frac{\rho_{NIR} - \rho_{SWIR}}{\rho_{NIR} + \rho_{SWIR}} \quad (2)$$

Where for MODIS, ρ_{blue} is the surface reflectance value in the blue (459-479 nm, band 3), ρ_{red} is the surface reflectance value in the red (621-670 nm, band 1), ρ_{NIR} is the surface reflectance value in the NIR (841-875 nm, band 2), and ρ_{SWIR} is the surface reflectance in the SWIR (1628-1652 nm, band 6). For OLI, ρ_{blue} , ρ_{red} , ρ_{NIR} and ρ_{SWIR} are associated to channel 2 (452-512 nm), channel 4 (636-673 nm), channel 5 (851-879 nm), and channel 6 (1570-1650 nm). a , b , c and d constants equal to 2.5, 6, 7.5 and 1, respectively, for both MODIS and OLI (USGS, product guide).

To process multispectral images, the first step consists in removing the cloud-contaminated pixels applying a cloud masking based on a threshold of the surface reflectance in the blue band ($\rho_{\text{blue}} \geq 0.2$). Then, spectral indices are computed. Note that, contrary to (Sakamoto et al., 2007), no smoothing was applied on spectral indices time-series. In a second step, the identification of the status of each pixel is performed applying thresholds on EVI, LSWI and their differences (Figure 2), which reduce the noise component. Thresholds determined by Sakamoto et al. (2007) were validated for our study site using ~~the MODIS and~~ OLI images acquired on ~~0401/07/2013 and 0402/0708/2013~~ and compared to MODIS respectively (Figure S13). Histograms show a similar bi-modal distribution for both EVI, LSWI and EVI-LSWI between MODIS and OLI 500 m (Figure 3-S1 and 4-S2). For EVI, pixels with a value lower than 0.1 are clearly associated with water land surfaces, while pixels with a value higher than 0.3 are associated with soil and vegetation features. Other pixels, with an EVI value comprised between 0.1 and 0.3, are identified as mixed surface types. For LSWI, pixels with a value higher than 0.5 are clearly associated with water land surfaces, while pixels with a value lower than 0.3 are associated with vegetation features or soil land surfaces when LSWI values are negative. Other pixels, with an LSWI value comprised between 0.3 and 0.5, are identified as mixed surface types. Contrary to what was found by Sakamoto et al. (2007) in the Mekong Basin, no negative value of LSWI were observed over our study area. This threshold was not applied in this study. For EVI-LSWI, pixels with a value lower than -0.05 are represented water land surface and values comprised between -0.05 and 0.1 are associated to ~~mixture~~mixed pixels. Other pixels, with values higher than 0.1 are represented vegetation features or soil land surfaces (Figure-S24). Each pixel was then classified in two main categories: non-flooded ($\text{EVI} > 0.3$ or $\text{EVI} \leq 0.3$ but $\text{EVI} - \text{LSWI} > 0.05$) and water-influenced ($\text{EVI} \leq 0.3$ and $\text{EVI} - \text{LSWI} \leq 0.05$ or $\text{EVI} \leq 0.05$) (Figure 2). The second category was divided into three sub-classes: mixed pixels ($0.1 < \text{EVI} \leq 0.3$), flooded pixels ($\text{EVI} \leq 0.1$) and permanent water bodies (e.g. lake, river and sea), when the total duration of a pixel classified as flooded is longer than 70 days out of 105 day for the study period. This ~~annual-total~~ duration for our study correspond roughly to 2/3 of the study period, as proposed by Sakamoto et al. (2007). The spatio-temporal variations of floods have been characterized for the months included between June and September over the 2000-2015 period.

Thereafter, we define in this paper land water surface as permanent water bodies with flooded areas although inundated surfaces including only inundated areas.

4.2 Validation of MODIS retrievals using OLI

Evaluation of the performance of the land water surface detection from MODIS is based on the comparison between land surface water estimated from MODIS at a 500 m-resolution, OLI at a 30 m-resolution, and OLI re-sampled at 500 m-resolution. For the validation purpose, MODIS and OLI images are selected when (1) the time-difference between the acquisitions of two satellite images is lower than 3 days and (2) the presence of cloud over the area is lower than 5%. Following these criteria, only two cloud-free OLI composites were selected between 1st July 2013 and 2nd August 2013.

4.3 Satellite-derived water level time-series in the Mackenzie Delta

The concept of radar altimetry is explained below. The radar emits an electromagnetic (EM) wave towards the surface and measures the round-trip time (Δt) of the EM wave. Taking into account propagation corrections caused by delays due to the interactions of electromagnetic wave in the atmosphere, and geophysical corrections, the

height of the reflecting surface (h) with reference to an ellipsoid can be estimated as (Créaux et al., submitted2017):

$$h = H - (R + \sum \Delta R_{\text{propagation}} + \Delta R_{\text{geophysical}}) \quad (3)$$

where H is the satellite center of mass height above the ellipsoid, R is the nadir altimeter range from the satellite center of mass to the the surface taking into account instrument corrections ($R = c\Delta t/2$ where c is the light velocity in the vacuum), $\sum \Delta R_{\text{propagation}}$ is the sum of the geophysical and environmental corrections applied to the range, respectively.

$$\sum \Delta R_{\text{propagation}} = \Delta R_{\text{ion}} + \Delta R_{\text{dry}} + \Delta R_{\text{wet}} \quad (4)$$

where ΔR_{ion} is the atmospheric refraction range delay due to the free electron content associated with the dielectric properties of the ionosphere, ΔR_{dry} is the atmospheric refraction range delay due to the dry gas component of the troposphere, ΔR_{wet} is the atmospheric refraction range delay due to the water vapor and the cloud liquid water content of the troposphere.

$$\sum \Delta R_{\text{geophysical}} = \Delta R_{\text{solid Earth}} + \Delta R_{\text{pole}} \quad (5)$$

Where $\Delta R_{\text{solid Earth}}$ and ΔR_{pole} are the corrections respectively accounting for crustal vertical motions due to the solid Earth and pole tides. The propagation corrections applied to the range are derived from model outputs: the Global Ionospheric Maps (GIM) and Era Interim from the European Centre Medium-Range Weather Forecasts (ECMWF) for the ionosphere and the dry and wet troposphere range delays respectively. The changes of the altimeter height h over the hydrological cycles are related to variations in water level. Here, the Multi-mission altimetry Processing Software (MAPS) was used to precisely select valid altimetry data at every virtual station locations (see part 3.3) series in the Mackenzie Delta (Frappart et al., 2015b). Data processing consists in four steps (Frappart et al., 2015b):

- The rough delineation of the river/lake cross-sections with overlaying altimeter tracks using Google Earth. Distances of plus or minus 5 km from the river banks are generally considered.
- The loading of the altimetry over the study area and the computation of the altimeter heights from the raw data contained in the GDRs,
- Valid altimetry data were selected through a refined process that consists in eliminating: ~~o~~Outliers and measurements over non-water surfaces ~~are delete~~, based on visual inspection. The shape of the altimeter along-track profiles permit to identify the river that is generally materialized as a shape of “V” or “U” with the lower elevations corresponding to the water surface (see Santos da Silva et al., 2010 and Baup et al., 2014 for more details).
- The computation of the time-series of water level.

4.4 Surface water volume storage

The approach used to estimate the anomalies of surface water volume is based on the combination of the surface water extent derived from MODIS images with altimetry-based water levels estimated at virtual stations distributed all over the delta (Figure 56). Surface water level maps were computed from the interpolation of water levels over the land water surfaces using an inverse-distance weighting spatial interpolation technique following (Frappart et al., 2012). Hence, water level maps were produced every 8 days from 2000 to 2015. For each water pixel, the minimal height of water during 2000-2015 is estimated. As ERS-2, ENVISAT and SARAL had a repeat cycle of 35 days, water levels are linearly interpolated every 8 days to be combined with the MODIS composite images.

Surface water volume time series are estimated over the Mackenzie Delta following (Frappart et al., 2012):

$$V = \sum_{j \in S} [h(\lambda_j, \varphi_j) - h_{\min}(\lambda_j, \varphi_j)] \cdot \delta_j \cdot \Delta S \quad (6)$$

Where V is the anomaly of surface water volume (km^3), S is the surface of the Mackenzie Delta (km^2), $h(\lambda_j, \varphi_j)$ the water level, $h_{\min}(\lambda_j, \varphi_j)$ the minimal water level for the pixel of coordinates (λ_j, φ_j) inside the Mackenzie Delta, δ_j equals 1 if the j^{th} pixel is associated to permanent water body/inundated and 0 if not and ΔS the pixel surface (0.25 km^2).

5. Results and discussion

5.1 MODIS-based land water extent and their validation

Following Sakamoto et al. (2007) method, all pixels of 8-day image have been classified into 4 classes: class 0 corresponding to vegetation, class 1 to permanent water, class 2 to inundation and class 3 to mixture of land and water. Map of annual average of land water surface, composed of inundated and permanent water bodies (classes 1 and 2), was obtained at spatial and temporal resolutions of 500 m and 8 days respectively from June to September over the 2000-2015 period (Figure 35a). Map of annual average of land water surface duration along with associated standard deviation over 2000-2015 during ice-free period of three months and half (105 days) is presented in Figure 5b3b. Permanent water bodies (i.e., identified as land water surface more than 70 days annually) are located along the Mackenzie River main channel, its tributaries (Reindeer, Peel, Middle and East Channels) and major lakes of the Delta. The longer water areas (i.e., identified as flooded between 30 and 70 days annually) are surrounding permanent water bodies. Other areas of the delta are annually inundated up to 30 days (Figure 5a3a). The map of standard deviation of the annual flood duration shows ranges from a few days over the areas affected by floods during a short time span to 15 days close to permanent water bodies (Figure 5b3b). Maps of errors made on land water surface duration with associated standard deviation are shown in Figure 5e-3c and 5d-3d over 2000-2015. Mixture-Mixed pixels have been used to calculate the error for each pixel the error on land water surface duration, corresponding to the class 3 “mixture” of Sakamoto et al., 2007 classification. Standard deviation of error is presented in Figure 5d3d. Maximal error and error standard deviation is obtained for pixels of potential flooding area in the delta. If short differences – lower than 20 ± 12 days – can be observed in the downstream part of the delta (over 69°N), longer differences (30 to 50 ± 15 to 20 days) are present in the upstream part. They can be attributed to the presence of small permanent lakes in this area (see the discussion on the validation of the surface water extent (see sub-section 5.2). Important interannual differences can be observed between wetter (Figure 3e) and dryer (Figure 3f) years with maximum annual inundation extent occurring in June and ranging from xxx in yyyy to xxx in yyyy (Figure 4). Important interannual differences can be observed between wetter (Figure 5e) and dryer (Figure 5f) years.

Maps of difference between the duration of extreme land water surface and the mean land water surface duration from 2000 to 2015 were estimated for the large historic flood that occurred in 2006 (Figure 35e) and for the minimal flood that occurred in 2010 (Figure 35f). The whole Mackenzie Delta was practically covered of water in 2006, whereas large areas, especially in the downstream part of the delta, were not inundated in 2010 (Figure 53f). Time series of land water surfaces of the Mackenzie Delta were derived from the 8-day maps of land water surface extent (Figure 46). Each year, water surface extent is maximum in June in response to the snow melt that occurred in May (between day of year, DOY, 110 and 130 on average) in the Delta and decreases to reach a minimum in

September, as previously observed by Goulding et al., 2009b, Goulding et al., 2009a. Land water surface extent varies from 1,500 to 14,284 km² between 2000 and 2015 along the hydrological cycle (Figure 46). On average, during the study period, maximum surface water extent is ~9,600 km². The largest water surface extent was reached in June 2006 with an inundated area of 14,284 km², which represents ~85% of the delta total surface (Figure 46). Large surface water extents (~12,500 km²) were also detected in 2011 and 2013 in accordance with high discharge peaks reported these years (<http://wateroffice.ec.gc.ca/>) and the historic inundation that occurred in Aklavik in 2006 (Beltaos and Carter, 2009).

5.2 Validation of land water surface

Surface water extent (the sum of permanent bodies and inundated areas) were also estimated applying the approach described in sub-section 3.1 for OLI images at 30 m of spatial resolution, and resampled at 500 m of spatial resolution. They were compared to MODIS-based surface water extent for the closest date (Table 1). Figure 7a-S3a, 7b-S3b and 7c-S3c present the maps of the surface water extent determined using MODIS, OLI 500 m and OLI 30 m respectively, acquired in July 2013. Medium and large scale (with a minimal size of 300 m) land water features are well detected as displayed on the zoomed part of images. Figure 7e-S3c present a zoom of surface water extent using OLI 30 m with permanent and inundated bodies. Surface water extent from OLI 500 m and MODIS are similar for both dates with differences lower than 20% (Table 1). For example in July 2013, land water surface is about 4,499 km² for OLI 500 and 3,798 km² for MODIS (Table 1). Percentages of common detection of surface water were estimated for the pixels detected as land water surface in the pair of satellite images. These percentages are 73 and 74 % for July 2013 and August 2013, respectively. Areas detected as water by both sensors corresponds to the main channels and connected floodplains. Differences appear on the boundaries of the commonly detected as inundated areas and at small-scales and can be attributed to the difference of acquisition dates between MODIS and OLI (Figure S4). These results highlight the robustness of the method of Sakamoto et al. (2007) for accurate land water surface retrievals. These surface water extent have been compared with surface water extent (channels and wetlands) determined by Emmerton et al. (2007) in Table 1. For MODIS, differences are lower than 15% and for OLI 500, differences are about 25% (Table 1).

However, the comparison between surface water extent estimated from OLI 30 m and MODIS 500 m shows important differences. In July 2013, surface water extent is about 3,798 km² from MODIS and 7,685 km² from OLI 30. The surface extents are higher for OLI 30 by a factor of 2 (Table 1). According to Emmerton et al., 2007, the Mackenzie Delta is composed of 49,000 lakes with a mean area of 0.0068 km² and 40% of the total number of lakes have an area inferior to 0.25 km². The pixel sizes of OLI 30 m and MODIS 500 m are approximately 0.0009 km² and 0.25 km², respectively. Thus, the high difference between the land water surfaces detected using OLI 30 m and MODIS is probably associated to a spatial sample bias. Small-scale water features detected from OLI cannot be detected from MODIS due to a lower spatial resolution.

Surface water extent determined using OLI 30 have been compared to Emmerton et al. (2007) surface water extent (including channels, wetlands and lakes). Emmerton et al., (2007) classified the Mackenzie Delta habitat in lakes, channels, wetlands and dry floodplains using information from a topographic maps derived from aerial photographs taken during the 1950's for low water periods. Differences between surface water extent of OLI 30 and Emmerton et al., (2007) are lower than 15 % (Table1).
~~and differences lower than 15 % are found (Table 1).~~

In order to investigate the assumption of spatial sample bias associated with MODIS 500 m, a satellite validation of surface water extent is performed (Table 2). Permanent water and inundated surfaces have been calculated for MODIS, OLI 500 and OLI 30. For OLI 30 and OLI 500, pixels identified as surface water for the two dates are considered as permanent waters (Table 2). In July 2013, inundated surfaces are nearly equal, about 577 km² for MODIS, 690 km² for OLI 500 and 627 km² for OLI 30 (Table 2). In August, inundated surfaces are equal to 250 km² and are 2.5 more important than OLI 30 (98 km²), if we consider OLI 30 as truth.

Time series of surface water extent in the Mackenzie Delta were derived from the 8-day maps of surface water extent (Figure 4). Surface extent water varies from 1,500 to 14,284 km² between 2000 and 2015 along the hydrological cycle. Each year, water surface extent is maximum in June in response to the spring ice break-up and snow melt that occurred in May (between day of year, DOY, 110 and 130 on average) in the Delta and decreases to reach a minimum in September, as previously observed by Goulding et al., 2009^{ba}, Goulding et al., 2009^{ab}. On average, during the study period, maximum surface water extent is ~9,600 km². The largest water surface extent was reached in June 2006 with an inundated area of 14,284 km², which represents ~85% of the delta total surface (Figure 4). Large surface water extents (~12,500 km²) were also detected in 2011 and 2013 in accordance with high discharge peaks reported these years (<http://wateroffice.ec.gc.ca/>) and the historic inundation that occurred in Aklavik in 2006 (Beltaos and Carter, 2009).

5.23 Alimetry-based water levels and their validation

The Mackenzie Delta is densely covered with altimetry tracks from the ERS-2, ENVISAT and SARAL missions that all were on the same nominal orbit. Twenty-two, twenty-seven and twenty-four altimetry virtual stations were built at the cross-section of an altimetry track with a water body for these three missions respectively (see Figure 8-5 for their locations). A water level temporal series is obtained for each virtual station.

The quality of altimetry-based water levels was evaluated using *in situ* gauge records. Only six virtual stations are located near *in situ* stations (with a distance lower than 20 km) for ERS-2 data, ten for ENVISAT and eight for SARAL data. Characteristics of these virtual stations are given in Table 3, s 3, 4 and 5 for ERS-2, ENVISAT and SARAL, respectively.

Altimetry-based water levels were validated using these virtual stations close enough (< 20 km) to *in situ* stations (6 comparisons for ERS-2, 10 for ENVISAT and 8 for SARAL). For ERS-2 and SARAL comparisons, the correlation *r* is low at the station 0114-c, i.e. -0.38 and 0.15 respectively (Table 3).

For ERS-2, quite high correlation coefficients are obtained for 4 virtual stations out of 6, with $r \geq 0.69$ and $RMS \leq 1$ m (Table 3). For the two other stations, no correlation is observed (-0.38 and 0.08 for ERS-2-0114c and ERS-2-0200-d respectively with a $RMS \geq 1$ m) (Table 3).

For ENVISAT, 8 out of 10 stations have a correlation coefficient ranging between 0.66 and 0.93 (Table 43). Except for ENV-0572-a, which is located 22 km away from the nearest *in situ* station, higher correlations were found when the river is larger at the VS (Table 43). For example, ENV-0114-b exhibits a negative correlation ($r = -0.27$) where the cross-section was only 150 m width (Table 43). This station is also located near the city of Inuvik. The presence of the town in the altimeter footprint could exert a strong impact on the radar echo and explain this low correlation.

For SARAL, 5 out of 6 virtual stations have a good correlation r coefficient higher than 0.76 with a low RMS (Table 53) due to its narrower footprint with an increase of the along-track sampling.

Comparisons between water levels derived from altimetry and *in-situ* are shown for two stations for ERS-2 (called ERS-2-0744-a and ERS-2-0439-a; Figure 9a-6a and 10a7a), three for ENVISAT (ENV-0744-a, ENV-0439-a and ENV-0028-a; in Figure 9b6b, 10b-7b and 118) and two for SARAL (SARAL-0744-a and SARAL-0439-a; Figure 9e-6c and 10e7c). Virtual station 0744-a is located in the downstream part of the delta, 0439-a in the center and 0028-a in the upstream part (Figure 58). For each station, water levels obtained by altimetry and water levels of *in situ* gauge are superposed (Figures 96, 10-7 and 118). Then, water level anomalies, which are computed as the average water level minus the water level, have been calculated for altimetry and in situ data.

The virtual station 0744-a is located in the North of the Mackenzie Delta (Figure 85). Water level time-series have been processed between 1995 and 2015 and compared to *in situ* data of the station 10MC010 for each mission ERS-2, ENVISAT and SARAL (Figure 96). *In situ* data are not continuous since river is frozen from October to April. With regard to altimetry, data have been acquired all the year but during frozen periods, water levels are unrealistic due to the presence of river ice. Thus, the processing is done only from the beginning of June to the end of September as for multispectral imagery treatment. The correlation r between altimetry water levels and in situ levels is 0.88 for ERS-2, 0.93 for ENVISAT and 0.99 for SARAL (Tables 3, 4 and 5). For the three missions, RMS is weak, lower than 0.15 m (Tables 3, 4 and 5). At this station, the variation of water level is about 2 m on average with an important water level in June that decreases to September (Figure 10a7a, 10e-7c and 10e7e).

The virtual station ERS-2-0439-a is in the center of the Mackenzie Delta and water levels time-series have been done between 1995 and 2015 and compared to *in situ* data of the station 10MC008 for the three missions ERS-2, ENVISAT and SARAL (Figure 107). The correlation between altimetry water levels and water levels from in situ gauge is about 0.76 for ERS-2, 0.89 for ENVISAT and 0.96 for SARAL (Tables 33, 4 and 5). RMS is included between 0.35 and 0.5 m for the three missions. On average at this station, water levels variations are about 4 meters with a maximal water level in June that decreases to reach a minimal value in September (Figure 10a7a, 10e-7c and 10e7e).

Water levels time-series between 2002 and 2010 at the virtual station ENV-0028-a located upstream of the Mackenzie Delta have been compared to *in situ* data of the station 10LC014 (Figure-811). A good correlation was found for this station too, with a coefficient correlation r of 0.83 and a RMS of 1.84 m (Table 43). For this station, variations of water levels are much higher with 9 m on average but reaching 12 m during the 2006 extreme event (Figure 11a8a). Water levels time-series were constructed have been done only for ENVISAT mission since for the two others (ERS-2 and SARAL), altimetry water levels were not consistent with exhibiting values around 70 meters. Therefore, water levels determined by altimetry and water level from *in situ* gauge have a difference, probably explained by the distance between virtual station and *in situ* gauge (16.31 km) since the slope is about - 0.02m/km in the Delta (Hill et al., 2001). Moreover, the seasonal cyclic thawing and freezing of the active layer causes cyclic settlement and heave at decimeters levels, estimated to 20 cm (Szostak-Chrzanowski, 2013).

To summarize, water levels time series were presented for three stations along the Mackenzie Delta (Figure 96, 10 7 and 118).

5.4.3 Time series of surface water storage anomalies in the Mackenzie Delta

The minimum water level of each inundated pixel was determined over the observation period. 8-day surface water levels maps were created after subtracting the minimum water level to water level at time t , using MODIS-based flood extent and altimetry-derived water levels in the entire delta from June to September. Example of water level maps are presented for 2006 at 4 different dates (in June, July, August and September), characterized as an historic flood (Figure 129).

Over the study period, water level maps show a realistic spatial pattern with a gradient of water level from south to north consistent with flow direction in the delta. On Figure 12a9a, in June 2006 for example, water levels are higher (about 5 m) upstream than downstream (about 0.5 m). The surface water storage reaches its maximal extent in June (Figure 12a9a) and then decreases during the following months, reaching 1 m in September in the entire delta (Figure 12b9b, 12e-9c and 12d9d).

The time series of surface water volume variations was estimated from 2000 to 2010 and then from 2013 to 2015, between June and September, following a similar approach as in Frappart et al., 2012 (Figure 1310). Surface water storage was estimated from 2000 to 2003 using ERS-2 data, from 2003 to 2010 using ENVISAT data and from 2013 to 2015 using SARAL. Between 2010 and 2013, surface water storage could not be estimated due to lack of RA data over the delta. ~~The time series of surface water volumes is presented in Figure 1310. We assess the~~ impact of the presence of a virtual station located in the upstream part of the delta and the inclusion of ERS-2 data on our satellite-based surface water volume estimation ~~were assessed~~. For ERS-2 and SARAL data, no virtual station was created in the upstream part due to unreliable water levels in the ~~upstream part of the delta~~. During the SARAL observation period, *in situ* water levels from 10LC014 station were used. One curve corresponds to surface water volume with virtual station in the upstream part of the delta (2002-2015; red) and another one without virtual station in the upstream part of the delta (2000-2015; green). Correlations between river discharges and surface water volumes with and without (2002-2015) upstream virtual station are the same (0.66). Of the presence of a virtual station in the upstream part of the Mackenzie decreases the water volume by $\sim 0.3 \text{ km}^3$ on average (Figure 1310). The correlation is lower (0.63) when ERS-2 data are included in the analysis (2000-2015). The integration of ERS-2 data have a lower accuracy slight decrease the correlation between water storage and flux.

In term of temporal variability, a clear seasonal cycle is visible with a yearly maximum of water surface volume occurring in June (about 9.7 km^3 on average), followed by a decrease until September (Figure 1310). The peak generally corresponds to the presence of the extensive flood covering the delta in June, and during summer, the volume decreases to reach its minimal in September ($\sim 0.2 \text{ km}^3$). The largest surface water volume happened in 2006 with a volume of 14.4 km^3 (Figure 1310), known as an historic flood (Beltaos and Carter, 2009). These results showed that the satellite-based surface water volumes estimation are consistent with the Mackenzie River discharge, which is the main driver of the delta flooding.

5.5 Validation

~~Our results were compared to the ones estimated by Emmerton et al. (2007) under the assumption of a storage change as a rectangular water layer added to the average low water volume for a stage variations from 1.231 m above sea level during low water period and 5.636 m above sea level at peak flood. Using this approach, Emmerton et al. (2007) found an increase in water volume of 14.14 km^3 over the floodplains and 7.68 km^3 over the channels.~~

With our method, maximal water volume is around 9.6 km^3 in average and can reach 14 km^3 . As it can be seen in Figure 11, water levels present a strong gradient over the delta and are, in average, lower than 5.636 m from Emmerton et al. (2007). The difference of approaches is likely to account for such discrepancy.

65. Discussion

65.1 Spatio-temporal dynamics of surface water extent

Maps of surface water extent duration for annual average from 2000 to 2015 exhibit important spatio-temporal variations along the Mackenzie Delta (Figure 3a). Areas with open water present during the whole study period are located along the Mackenzie River and its tributaries. On the contrary, areas covered with open water for a duration lower than 30 days on the study period of 120 days are mostly located in the western upstream and eastern downstream parts of the delta but also in some locations in the western downstream part and along the Mackenzie mainstream (Figure 3a). They correspond to regions only inundated in June during the floods caused by spring ice break-up and snow melt occurring in May (see Figure 9 for the temporality of the flood extent). The central part of the Mackenzie is inundated between 40 and 70 days per year (Figure 3a). As it can be seen in Figure 9, this area is not continuously inundated but during two flood events in June in response to snowmelt and in August and September in response to an increase of river discharges of the Mackenzie River. This secondary peak ranges from $3,000$ to $5,000 \text{ km}^2$ in comparison with the sooner one that ranges from $4,000$ to $10,000 \text{ km}^2$ (Figure 4).

Maps of difference between the duration of extreme surface water surface and the average duration water surface duration from 2000 to 2015 were estimated for the large historic flood that occurred in 2006 (Figure 3e) and for the minimal flood that occurred in 2010 (Figure 3f). The whole Mackenzie Delta was practically covered of water in 2006, whereas large areas, especially in the downstream part of the delta, were not inundated in 2010 (Figure 3f).

Time series of land water surfaces of the Mackenzie Delta were derived from the 8-day maps of land water surface extent (Figure 4). Each year, water surface extent is maximum in June in response to the snow melt that occurred in May (between day of year, DOY, 110 and 130 on average) in the Delta and decreases to reach a minimum in September, as previously observed by Goulding et al., 2009b, Goulding et al., 2009a. Land water surface extent varies from $1,500$ to $14,284 \text{ km}^2$ between 2000 and 2015 along the hydrological cycle (Figure 4). On average, during the study period, maximum surface water extent is $\sim 9,600 \text{ km}^2$. The largest water surface extent was reached in June 2006 with an inundated area of $14,284 \text{ km}^2$, which represents $\sim 85\%$ of the delta total surface (Figure 4). Large surface water extents ($\sim 12,500 \text{ km}^2$) were also detected in 2011 and 2013 in accordance with high discharge peaks reported these years (<http://wateroffice.ec.gc.ca/>) and the historic inundation that occurred in Aklavik in 2006 (Beltaos and Carter, 2009).

65.2 Spatio-Temporal dynamics of surface water levels in the Mackenzie delta

For all stations and RA missions, a strong seasonal cycle can be seen, with a maximum water level reach in June after the spring ice break-up and snow melt that decreases to reach a minimal value in September, in good accordance with the hydrological cycle of the Mackenzie Delta. The Delta is frozen from October to May and during spring-early summer, the freshwater meets an ice dam that was formed in winter, what provokes river discharges variations from $5,000 \text{ m}^3$ to $25,000 \text{ m}^3$ on average (<http://wateroffice.ec.gc.ca/>, Figure 1b). Then, these

important variations provoke water levels increase and important floods each year in the delta. However, water levels variations as revealed from RA are not equal over the delta. In the upstream part, variations are 9 m on average, 4 m in the center and 3 m in the downstream part of the Mackenzie Delta.

Water level time-series from data acquired by the ENVISAT mission between June and September averaged over 2002-2010 are presented in Figure 11. Each time-series has been shifted manually and errors are not shown here for clarity purpose. Virtual stations used to discuss the spatio-temporal variations were chosen along the Mackenzie River from upstream to downstream and at similar latitudes on the Mackenzie River and its tributaries. They are represented using green dots for variations along the Mackenzie River and red triangles for latitudinal variations (Figure 11a). Time-series from Figure 11b are located along the Mackenzie River, number 1 is corresponding to the upstream part and number 8 to the downstream part. Logically, a stronger seasonal cycle is observed upstream than downstream. If the primary peak of flood that occurs in June clearly appears for all the stations, the secondary peak of August-September is not well marked for all the stations. This could be due to either local differences in the hydrodynamics of the river or due to the low temporal frequency of acquisition of the altimeters that is not sufficient to fully capture the whole specificities of the hydrological cycle (see Biancamaria et al., 2017 for instance). Latitudinal differences can also be noticed (Figure 11c). Larger annual amplitudes of water levels can be observed in the Mackenzie River than over its tributaries. The second flood event occurs earlier in the central part (August) than in the western and eastern parts (September).

65.3 Spatio-temporal dynamics of surface water storage

The spatio-temporal dynamics of surface water storage is presented in Figure 9 for 2006. A strong upstream-downstream gradient of water levels can be observed in June with water levels ranging 0 to 5 m from north to south (Figure 9a). It strongly decreases in July (0 to 1.5 m in Figure 9b) and does not appear in August (Figure 9c) and September (Figure 9d). For these two later months differences in water levels are more homogeneous of the whole delta (except in a region located around 135°W and between 68°N and 68°30'N in August°). Our results were compared to the ones estimated by Emmerton et al. (2007) under the assumption of a storage change as a rectangular water layer added to the average low-water volume for a stage variation from 1.231 m above sea level during low water period and 5.636 m above sea level at peak flood. Using this approach, Emmerton et al. (2007) found an increase in water volume of 14.14 km³ over the floodplains and 7.68 km³ over the channels. With our method, maximal water volume is around 9.6 km³ in average and can reach 14 km³. As it can be seen in Figure 11, water levels present a strong decreasing gradient of amplitude over the delta towards the mouth and are, in average, lower than 5.636 m from Emmerton et al. (2007). The difference of approaches is likely to account for such discrepancy. The comparison between storage and flux (discharge) exhibits a quite good correlation ($R=0.66$ with no time-lag) between these two quantities. Several studies demonstrated that there is no linear relationship between surface water extent, surface water volume and river discharge due to the presence of floodplains non-connected to the river (e.g., Frappart et al., 2005; Heimhuber et al., 2017). Due to the small area of the non-connected lakes present in the Mackenzie delta, they are detected in our approach based on the use of MODIS images at 500 m of spatial resolution, as mixture areas (except during the June flood event where almost all the delta is inundated and

all the flooded areas are connected to the river). Only the floodplains connected to river are considered in this study.

Our results were compared to the ones estimated by Emmerton et al. (2007) under the assumption of a storage change as a rectangular water layer added to the average low water volume for a stage variations from 1.231 m above sea level during low water period and 5.636 m above sea level at peak flood. Using this approach, Emmerton et al. (2007) found an increase in water volume of 14.14 km³ over the floodplains and 7.68 km³ over the channels. With our method, maximal water volume is around 9.6 km³ in average and can reach 14 km³. As it can be seen in Figure 11, water levels present a strong decreasing gradient of amplitude over the delta towards the mouth and are, in average, lower than 5.636 m from Emmerton et al. (2007). The difference of approaches is likely to account for such discrepancy.

76. Conclusion

This study provides surface water estimates (permanent water of rivers, lakes large features and inundated surfaces connected to the rivers) dynamics both in extent and storage in the Mackenzie Delta from 2000 to 2015 using MODIS images at 500 m of spatial resolution and altimetry-based water levels. Surface water exhibits a maximal extent in the beginning of June and decreases to reach a minimal value in September. In June, the extent of land water surface is on average about 9,600 km². The highest value was observed in 2006 (~14,284 km²), during the historic flood described by (Beltaos and Carter, 2009). Despite the lower resolution of MODIS images in comparison with Landsat-8 ones, surface water extent estimates are quite similar using both sensors over the river channels and the floodplains with an underestimation of 20% is found for MODIS. But, the numerous large number of small lakes present in the Mackenzie Delta are is not detected using MODIS. Nevertheless, the MODIS-based inundation product provides important information on flooding patterns along the hydrological cycle (flood events of June and August-September).

Virtual stations, or river/lake cross-section have been created across the Mackenzie Delta for the three radar altimetry missions (ERS-2, 1993-2003; ENVISAT, 2002-2010; SARAL, since 2013). Due to the lack of valid data acquired in interferometry SAR mode by Cryosat-2, no information on surface water levels is available in 2011 and 2012. The water levels determined by altimetry at those stations have been validated with *in situ* river levels with good correlation coefficient (> 0.8) for the three missions. The dense network of altimetry virtual stations composed of 22 stations for ERS-2, 27 for ENVISAT and 24 for SARAL allowed the analysis of the spatio-temporal variations of water levels across the delta.

The combination between land water extent determined by MODIS imagery and the water levels derived from altimetry has permitted to calculate the estimate surface water volume storage variations in the Mackenzie Delta at 8-day temporal resolution. Maps of surface water levels showed a clear upstream-downstream gradient in June that decreases with time. Temporal variations in surface water volume calculated from 2000 to 2010 and from 2012 to 2015 showed a maximal volume in June (on average 9.6 km³) and a minimal volume in September (about 0.1 km³). A relatively strong correlation was found between surface water volume and the Mackenzie River discharges (R=0.66), suggesting that the latter is the main driver of the delta flooding. Overall these results indicate that the satellite-based water volume estimation are consistent and can be used to monitor the recurrent flooding of large Arctic deltas.

~~The recent launches of Sentinel 1, Sentinel 2 and 3 offer new opportunities for flood monitoring at higher spatial (~10 m) and temporal (a few days) resolutions. Besides, T~~these products provide a unique long-term dataset that allows a continuous monitoring of the changes affecting the surface water reservoir before the launch of the NASA-CNES Surface Water and Ocean Topography (SWOT) mission in 2021. This approach can be applied to any other deltaic and estuarine environments as MODIS and altimetry data are available globally. The major limitations are i) the presence of clouds and dense vegetation cover that prevent the use of MODIS images, ii) the relatively coarse spatial resolution of MODIS images, iii) the coarse coverage of altimetry tracks. They can be overcome i) using SAR images for flood extent monitoring as Frappart et al. (2005), ii) using images with a higher spatial resolution, iii) combining information the different altimetry missions orbiting simultaneously. ~~The recent launches of Sentinel-1, Sentinel-2 and 3 offer new opportunities for flood extent monitoring at higher spatial (from ~10 m to 300 m) and temporal (a few days) resolutions.~~ Associated with Aquatic color radiometry (Mouw et al., 2015), the approach developed here should provide useful information for the study of fluvial particle transport along the river-to-coastal ocean continuum and its potential impacts on ecosystems.

7. Acknowledgments

This study was supported by an internship grant from LabEX Côte (Université de Bordeaux) and a PhD grant from Ministère de l'Enseignement Supérieur et de la Recherche and also by the CNES TOSCA CTOH ~~and the CNES OSTST FOAM~~ grants. The authors also thank David Doxaran for fruitful discussion.

References

Alsdorf, D. E., Rodríguez, E. and Lettenmaier, D. P.: Measuring surface water from space, Rev. Geophys., 45(2), RG2002, doi:10.1029/2006RG000197, 2007.

~~Are, F. and Reimnitz, E.: An overview of the Lena River Delta setting: geology, tectonics, geomorphology, and hydrology. Journal of Coastal Research, 16(4), 1083–1093. West Palm Beach (Florida), ISSN 0749-02, 2000.~~

Baup, F., Frappart, F. and Maubant, J.: Combining high-resolution satellite images and altimetry to estimate the volume of small lakes. Hydrol. Earth Syst. Sci., 18, 2007–2020, doi:10.5194/hess-18-2007-2014, 2014.

~~Beltaos, S.: Hydrodynamic and climatic drivers of ice breakup in the lower Mackenzie River, Cold Reg. Sci. Technol., 95, 39–52, doi:10.1016/j.coldregions.2013.08.004, 2013.~~

Beltaos, S. and Carter, T.: Field studies of ice breakup and jamming in the Mackenzie Delta, St John's, Newfoundland and Labrador., 2009.

Beltaos, S., Carter, T. and Rowsell, R.: Measurements and analysis of ice breakup and jamming characteristics in the Mackenzie Delta, Canada, Cold Reg. Sci. Technol., 82, 110–123, doi:10.1016/j.coldregions.2012.05.013, 2012.

Biancamaria, S., Frappart, F., Leleu, A.-S., Marieu, V., Blumstein, D., Desjonquères, J.-D., Boy, F., Sottolichio, A. and Valle-Levinson A.: Satellite radar altimetry elevations performance over a 200 m wide river: Evaluation over the Garonne River, Advances in Space Research, 59, 128–146, 2017.

Birkett C.M.: The contribution of TOPEX/POSEIDON to the global monitoring of climatically sensitive lakes. Journal of Geophysical Research, 100, 179–204, 1995.

~~Bullock A., Acreman M.: The role of wetlands in the hydrological cycle. Hydrol. Earth Syst. Sci, 7, 358–389, 2003.~~

Cazenave, A., Bonnefond, P., Dominh, K. and Schaeffer, P.: Caspian sea level from Topex-Poseidon altimetry: Level now falling, *Geophys. Res. Lett.*, 24(8), 881–884, doi:10.1029/97GL00809, 1997.

~~Carmack, E. C., and R. W. MacDonald.: Oceanography of the Canadian Shelf of the Beaufort Sea: A setting for Marine Life. *Arctic*, 55(1), 29–45, 2002.~~

- 5 Crétaux, J.-F., Jelinski, W., Calmant, S., Kouraev, A., Vuglinski, V., Bergé-Nguyen, M., Gennero, M.-C., Nino, F., Abarca Del Rio, R., Cazenave, A. and Maisongrande, P.: SOLS: A lake database to monitor in the Near Real Time water level and storage variations from remote sensing data, *Adv. Space Res.*, 47(9), 1497–1507, doi:10.1016/j.asr.2011.01.004, 2011.
- 10 Crétaux, J.-F., Bergé-Nguyen, M., Leblanc, M. and Abarca Del Rio, R.: FLOOD MAPPING INFERRED FROM REMOTE SENSING DATA., ~~n.d.~~ [n.d. 2017](#).
- Crétaux J.F., Nielsen K., Frappart F., Papa F., Calmant S., Benveniste J. Submitted. Hydrological applications of satellite altimetry: rivers, lakes, man-made reservoirs, inundated areas. *Satellite Altimetry Over Oceans and Land Surfaces*, Detlef Stammer, Anny Cazenave (Eds), ~~2017~~ [CRC Press](#)
- 15 Emmerton, C. A., Lesack, L. F. W. and Marsh, P.: Lake abundance, potential water storage, and habitat distribution in the Mackenzie River Delta, western Canadian Arctic: MACKENZIE DELTA WATER STORAGE, *Water Resour. Res.*, 43(5), n/a-n/a, doi:10.1029/2006WR005139, 2007.
- Emmerton, C. A., Lesack, L. F. W. and Vincent, W. F.: Nutrient and organic matter patterns across the Mackenzie River, estuary and shelf during the seasonal recession of sea-ice, *J. Mar. Syst.*, 74(3–4), 741–755, doi:10.1016/j.jmarsys.2007.10.001, 2008.
- 20 [Frappart, F., Seyler, F., Martinez, J.M., León, J.G., Cazenave, A.: Floodplain water storage in the Negro River basin estimated from microwave remote sensing of inundation area and water levels, *Remote Sens. Environ.*, 99, 387–399, doi:10.1016/j.rse.2005.08.016, 2005.](#)
- 25 Frappart, F., Calmant, S., Cauhope, M., Seyler, F. and Cazenave, A.: Preliminary results of ENVISAT RA-2-derived water levels validation over the Amazon basin, *Remote Sens. Environ.*, 100(2), 252–264, doi:10.1016/j.rse.2005.10.027, 2006a.
- Frappart, F., Minh, K. D., L’Hermitte, J., Cazenave, A., Ramillien, G., Le Toan, T. and Mognard-Campbell, N.: Water volume change in the lower Mekong from satellite altimetry and imagery data, *Geophys. J. Int.*, 167(2), 570–584, doi:10.1111/j.1365-246X.2006.03184.x, 2006b.
- 30 Frappart, F., Papa, F., Güntner, A., Werth, S., Ramillien, G., Prigent, C., Rossow, W. B. and Bonnet, M.-P.: Interannual variations of the terrestrial water storage in the Lower Ob’ Basin from a multisatellite approach, *Hydrol. Earth Syst. Sci.*, 14(12), 2443–2453, doi:10.5194/hess-14-2443-2010, 2010.
- Frappart, F., Papa, F., Santos da Silva, J., Ramillien, G., Prigent, C., Seyler, F. and Calmant, S.: Surface freshwater storage and dynamics in the Amazon basin during the 2005 exceptional drought, *Environ. Res. Lett.*, 7(4), 044010, doi:10.1088/1748-9326/7/4/044010, 2012.
- 35 Frappart, F., Papa, F., Malbeteau, Y., León, J., Ramillien, G., Prigent, C., Seoane, L., Seyler, F. and Calmant, S.: Surface Freshwater Storage Variations in the Orinoco Floodplains Using Multi-Satellite Observations, *Remote Sens.*, 7(1), 89–110, doi:10.3390/rs70100089, 2015a.
- Frappart, F., Papa, F., Marieu, V., Malbeteau, Y., Jordy, F., Calmant, S., Durand, F. and Bala, S.: Preliminary Assessment of SARAL/AltiKa Observations over the Ganges-Brahmaputra and Irrawaddy Rivers, *Mar. Geod.*, 38(sup1), 568–580, doi:10.1080/01490419.2014.990591, 2015b.
- 40 Frappart, F., Legrésy, B., Niño, F., Blarel, F., Fuller, N., Fleury, S., Birol, F. and Calmant, S.: An ERS-2 altimetry reprocessing compatible with ENVISAT for long-term land and ice sheets studies, *Remote Sens. Environ.*, 184, 558–581, doi:10.1016/j.rse.2016.07.037, 2016.
- 45 Fu, L.-L. and Cazenave, A., Eds.: *Satellite altimetry and earth sciences: a handbook of techniques and applications*, Academic Press, San Diego., 2001.

- Goulding, H. L., Prowse, T. D. and Bonsal, B.: Hydroclimatic controls on the occurrence of break-up and ice-jam flooding in the Mackenzie Delta, NWT, Canada, *J. Hydrol.*, 379(3–4), 251–267, doi:10.1016/j.jhydrol.2009.10.006, 2009a.
- 5 Goulding, H. L., Prowse, T. D. and Beltaos, S.: Spatial and temporal patterns of break-up and ice-jam flooding in the Mackenzie Delta, NWT, *Hydrol. Process.*, 23(18), 2654–2670, doi:10.1002/hyp.7251, 2009b.
- [Heimhuber, V., Tulbure, M.G. and Broich, M.: Modeling multidecadal surface water inundation dynamics and key drivers on large river basin scale using multiple time series of Earth-observation and river flow data, *Water Resources Research*, 53, 1251–1269, doi:10.1002/2016WR019858, 2017.](#)
- 10 Hill, P. R., Lewis, C. P., Desmarais, S., Kauppaymuthoo, V. and Rais, H.: The Mackenzie Delta: sedimentary processes and facies of a high-latitude, fine-grained delta, *Sedimentology*, 48(5), 1047–1078, doi:10.1046/j.1365-3091.2001.00408.x, 2001.
- 15 Holmes, R. M., McClelland, J. W., Peterson, B. J., Tank, S. E., Bulygina, E., Eglinton, T. I., Gordeev, V. V., Gurtovaya, T. Y., Raymond, P. A., Repeta, D. J., Staples, R., Striegl, R. G., Zhulidov, A. V. and Zimov, S. A.: Seasonal and Annual Fluxes of Nutrients and Organic Matter from Large Rivers to the Arctic Ocean and Surrounding Seas, *Estuaries Coasts*, 35(2), 369–382, doi:10.1007/s12237-011-9386-6, 2012.
- Huete A.R., Liu H.Q., Batchily K. and van Leeuwen W.: A comparison of vegetation indices over a global set of TM images for EOS-MODIS. *Remote Sens. Environ.* 59, 440–451, 1997.
- ~~Kääb, A. and Prowse, T.: Cold regions river flow observed from space: COLD REGIONS RIVER FLOW FROM SPACE, *Geophys. Res. Lett.*, 38(8), n/a–n/a, doi:10.1029/2011GL047022, 2011.~~
- 20 ~~Kuenzer, C., Klein, I., Ullmann, T., Georgiou, E., Baumhauer, R. and Dech, S.: Remote Sensing of River Delta Inundation: Exploiting the Potential of Coarse Spatial Resolution, Temporally Dense MODIS Time Series, *Remote Sens.*, 7(7), 8516–8542, doi:10.3390/rs70708516, 2015.~~
- [Klein, I., Gessner, U., Dietz, A.J., Kuenzer, C.: Global WaterPack - A 250 m resolution dataset revealing the daily dynamics of global inland water bodies. *Remote Sens. Environ.*, 198, 345–362, doi.org/10.1016/j.rse.2017.06.045, 2017.](#)
- 25 Lesack, L. F. W. and Marsh, P.: River-to-lake connectivities, water renewal, and aquatic habitat diversity in the Mackenzie River Delta: RIVER-TO-LAKE WATER CONNECTIVITIES, *Water Resour. Res.*, 46(12), n/a–n/a, doi:10.1029/2010WR009607, 2010.
- 30 Macdonald, R. W. and Yu, Y.: The Mackenzie Estuary of the Arctic Ocean, in *Estuaries*, vol. 5H, edited by P. J. Wangersky, pp. 91–120, Springer-Verlag, Berlin/Heidelberg. [online] Available from: http://link.springer.com/10.1007/698_5_027 (Accessed 14 December 2016), 2006.
- ~~Maltby, E.: Wetland management goals: Wise use and conservation. *Landsc. Urban Plan.*, 20, 9–18, 2003.~~
- ~~Marsch, P.: Lakes and water in the Mackenzie Delta, Scientific report, Aurora research institute. 1998.~~
- 35 Mouw, C. B., Greb, S., Aurin, D., DiGiacomo, P. M., Lee, Z., Twardowski, M., Binding, C., Hu, C., Ma, R., Moore, T., Moses, W. and Craig, S. E.: Aquatic color radiometry remote sensing of coastal and inland waters: Challenges and recommendations for future satellite missions, *Remote Sens. Environ.*, 160, 15–30, doi:10.1016/j.rse.2015.02.001, 2015.
- Muhammad, P., Duguay, C. and Kang, K.-K.: Monitoring ice break-up on the Mackenzie River using MODIS data, *The Cryosphere*, 10(2), 569–584, doi:10.5194/tc-10-569-2016, 2016.
- 40 ~~Nguyen, T. N., Burn, C. R., King, D. J. and Smith, S. L.: Estimating the extent of near surface permafrost using remote sensing, Mackenzie Delta, Northwest Territories, *Permafr. Periglac. Process.*, 20(2), 141–153, doi:10.1002/ppp.637, 2009.~~

~~Organisation for Economic Cooperation and Development. Guidelines for Aid Agencies for Improved Conservation and Sustainable Use of Tropical and Sub-tropical Wetlands; Guidelines Aid Environment: Paris, France, 1996.~~

Ogilvie, A., Belaud, G., Delenne, C., Bailly, J.-S., Bader, J.-C., Oleksiak, A., Ferry, L. and Martin, D.: Decadal monitoring of the Niger Inner Delta flood dynamics using MODIS optical data, *J. Hydrol.*, 523, 368–383, doi:10.1016/j.jhydrol.2015.01.036, 2015.

Papa, F., Prigent, C., Aires, F., Jimenez, C., Rossow, W.B. and Matthews E.: Interannual variability of surface water extent at the global scale, 1993-2004., *Journal of geophysical research*, 115, D12111, doi:10.1029/2009JD012674, 2010.

~~Pavelsky, T. M. and Smith, L. C.: Spatial and temporal patterns in Arctic river ice breakup observed with MODIS and AVHRR time series, *Remote Sens. Environ.*, 93(3), 328–338, doi:10.1016/j.rse.2004.07.018, 2004.~~

Pekel, J. F., Vancutsem, C., Bastin, L., Clerici, M., Vanbogaert, E., Bartholomé, E. and Defourny, P.: A near real-time water surface detection method based on HSV transformation of MODIS multi spectral time series data, *Remote Sens. Environ.*, 140, 704–716, doi:10.1016/j.rse.2013.10.008, 2014.

Pekel, J., Cottam, A., Gorelick, N., and Belward, A.S.: High resolution mapping of global surface water and its long-term changes, *Nature*, 540, 418–422, doi:10.1038/nature20584, 2016

Peterson, B. J., Holmes, R. M., McClelland, J. W., Vörösmarty, C. J., Lammers, R. B., Shiklomanov, A. I., Shiklomanov, I. A. and Rahmstorf, S.: Increasing River Discharge to the Arctic Ocean, *Science*, 298(5601), 2171–2173, doi:10.1126/science.1077445, 2002.

~~Pithan, F. and Mauritsen, T.: Arctic amplification dominated by temperature feedbacks in contemporary climate models, *Nat. Geosci.*, 7(3), 181–184, doi:10.1038/ngeo2071, 2014.~~

Rees W.G.: Physical principles of remote sensing, Cambridge University press, 460 p, 2013.

Sakamoto, T., Van Nguyen, N., Kotera, A., Ohno, H., Ishitsuka, N. and Yokozawa, M.: Detecting temporal changes in the extent of annual flooding within the Cambodia and the Vietnamese Mekong Delta from MODIS time-series imagery, *Remote Sens. Environ.*, 109(3), 295–313, doi:10.1016/j.rse.2007.01.011, 2007.

Santos da Silva, J., Calmant, S., Seyler, F., Rotunno Filho, O. C., Cochonneau, G. and Mansur, W. J.: Water levels in the Amazon basin derived from the ERS 2 and ENVISAT radar altimetry missions, *Remote Sens. Environ.*, 114(10), 2160–2181, doi:10.1016/j.rse.2010.04.020, 2010.

Smith, L. C.: Satellite remote sensing of river inundation area, stage, and discharge: a review, *Hydrol. Process.*, 11(10), 1427–1439, doi:10.1002/(SICI)1099-1085(199708)11:10<1427::AID-HYP473>3.0.CO;2-S, 1997.

Squires, M. M., Lesack, L. F. W., Hecky, R. E., Guildford, S. J., Ramlal, P. and Higgins, S. N.: Primary Production and Carbon Dioxide Metabolic Balance of a Lake-Rich Arctic River Floodplain: Partitioning of Phytoplankton, Epilong, Macrophyte, and Epiphyton Production Among Lakes on the Mackenzie Delta, *Ecosystems*, 12(5), 853–872, doi:10.1007/s10021-009-9263-3, 2009.

~~Seyler, F., Calmant, S., da Silva, J., Filizola, N., Roux, E., Cochonneau, G., Vauchel, P. and Bonnet, M. P.: Monitoring water level in large trans boundary ungauged basins with altimetry: the example of ENVISAT over the Amazon basin, edited by R. J. Frouin, S. Andrefouet, H. Kawamura, M. J. Lynch, D. Pan, and T. Platt, p. 715017., 2008.~~

Stocker, T. F. and Raible, C. C.: Water cycles shifts gear, *Nature*, 434, 2005.

Szostak-Chrzanowski, A.: Study of Natural and Man-induced Ground Deformation in MacKenzie Delta Region, *Acta Geodyn. Geomater.*, 1–7, doi:10.13168/AGG.2013.0060, 2013.

Tulbure, M.G., Broich, M., Stehman, S.V., Kommareddy A.: Surface water extent dynamics from the three decades of seasonally continuous Landsat time series at subcontinental scale in a semi-arid region. *Remote Sens. Environ.*, 178, 142-157, doi.org/10.1016/j.rse.2016.02.034, 2016.

Ulaby, F. T., Moore, R. K. and Fung, A. K.: Microwave remote sensing: Active and passive. Volume 1 - Microwave remote sensing fundamentals and radiometry. [online] Available from: <https://ntrs.nasa.gov/search.jsp?R=19820039342> (Accessed 15 December 2016), 1981.

5 U.S. Geological Survey. Product guide, Landsat surface reflectance-derived spectral indices. Version 3.3. December 2016.

Verpoorter, C., Kutser, T., Seekell, D. A. and Tranvik, L. J.: A global inventory of lakes based on high-resolution satellite imagery, *Geophys. Res. Lett.*, 41(18), 6396–6402, doi:10.1002/2014GL060641, 2014.

10 Verron, J., Sengenès, P., Lambin, J., Noubel, J., Steunou, N., Guillot, A., Picot, N., Coutin-Faye, S., Sharma, R., Gairola, R. M., Murthy, D. V. A. R., Richman, J. G., Griffin, D., Pascual, A., Rémy, F. and Gupta, P. K.: The SARAL/AltiKa Altimetry Satellite Mission, *Mar. Geod.*, 38(sup1), 2–21, doi:10.1080/01490419.2014.1000471, 2015.

Wang, M. and Shi, W., ~~2005~~. Estimation of ocean contribution at the MODIS near-infrared wavelengths along the east coast of the U.S.: Two case studies. *Geophys. Res. Lett.*, 32, L13606, ~~2005~~.

15 Xiao, X., Boles, S., Liu, J., Zhuang, D., Froking, S., Li, C., Salas, W., Moore, B., ~~2005~~. Mapping paddy rice agriculture in southern China using multi-temporal MODIS images. *Remote Sens. Environ.* 95, 480–492. doi:10.1016/j.rse.2004.12.009, ~~2005~~

Zelli C.: ENVISAT RA-2 Advances Radar Altimeter: instrument design and pre-launch performance assessment review. *Acta Astronautica*. 44, 323-33, 1999.

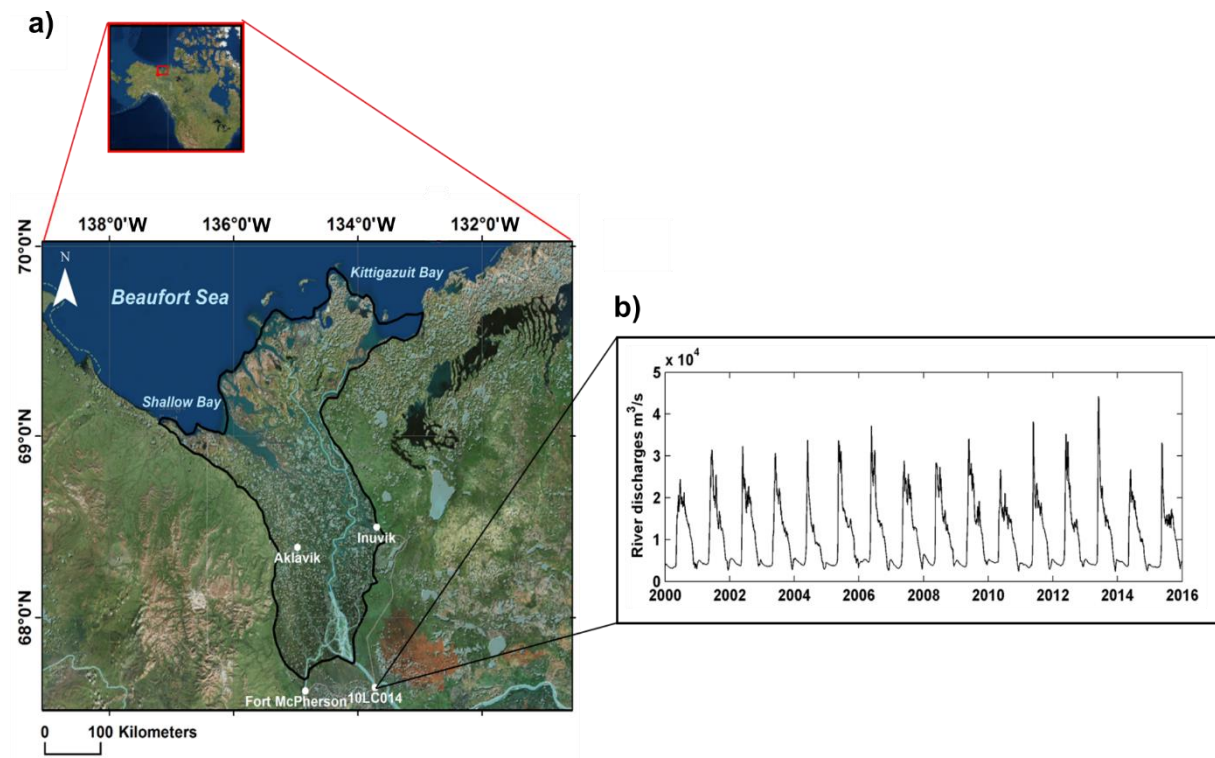


Figure 1: (a) Location of the Mackenzie Delta at the mouth of the Mackenzie River in the Northwest Territories of Canada (b) river discharges of the Mackenzie River at 10LC014 station from 2000 to 2015 (133°W, 67°N), 30 km upstream the Mackenzie Delta.

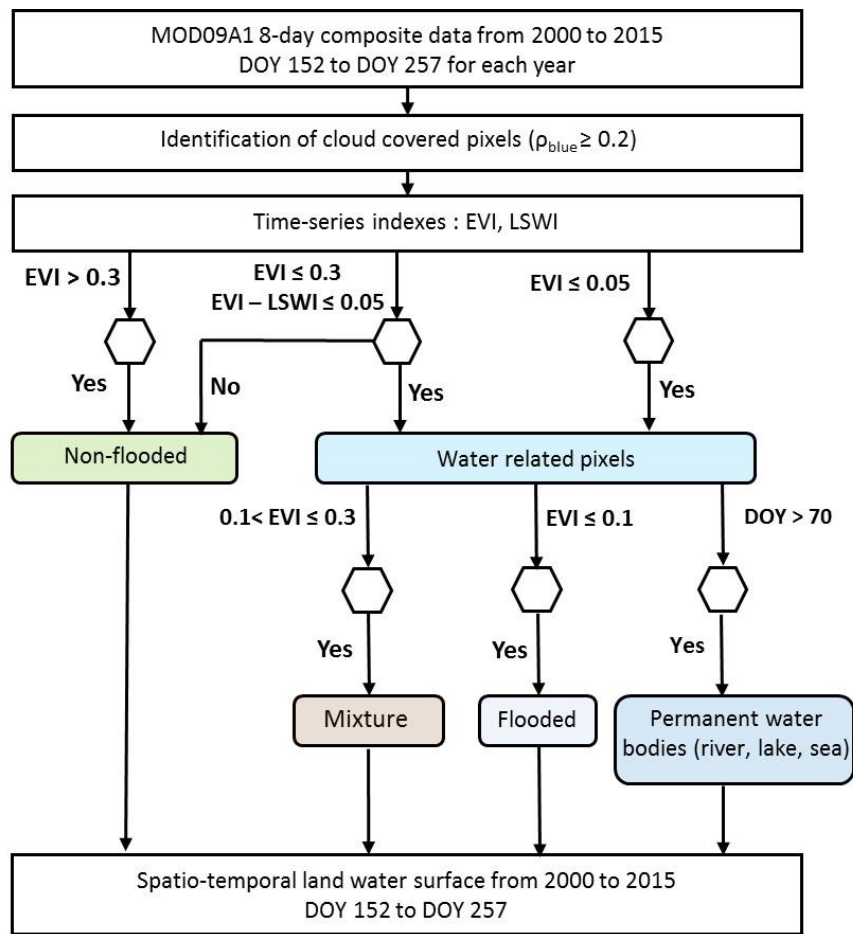


Figure 2142: Flow-chart of the method (adapted from Sakamoto et al., 2007) used to classify each pixel of the multispectral images acquired over the Mackenzie Delta in 4 categories (non-flooded, ~~mixture~~^{remixed}, flooded and permanent water bodies) for each year from 2000 to 2015 using MODIS 8-day composite data from the day of the year (DOY) 169 to 257.

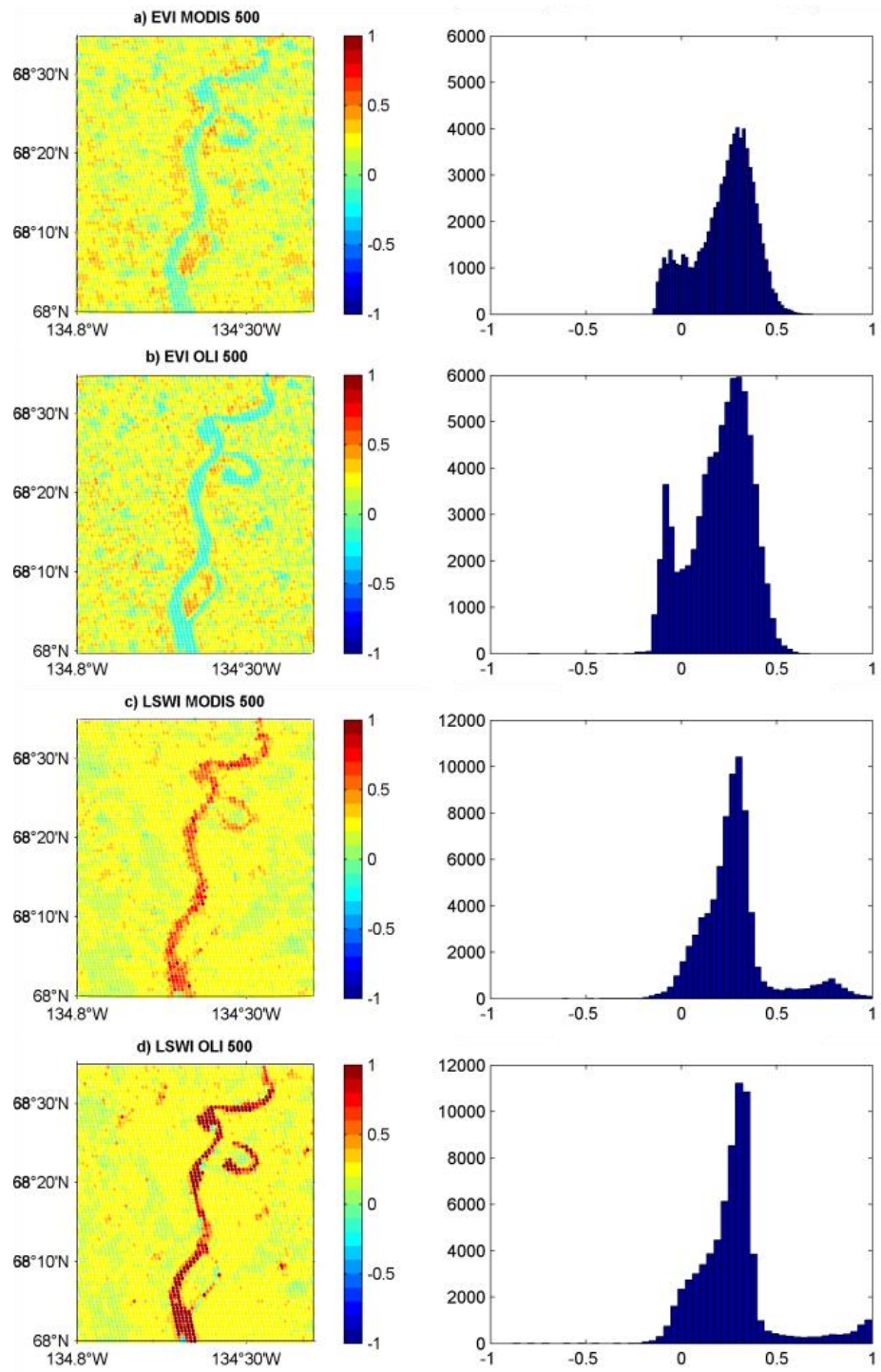


Figure 3: Index map and associated histogram in July 2013 for (a) EVI for MODIS, (b) EVI for OLI 500, (c) LSWI for MODIS and (d) LSWI for OLI 500

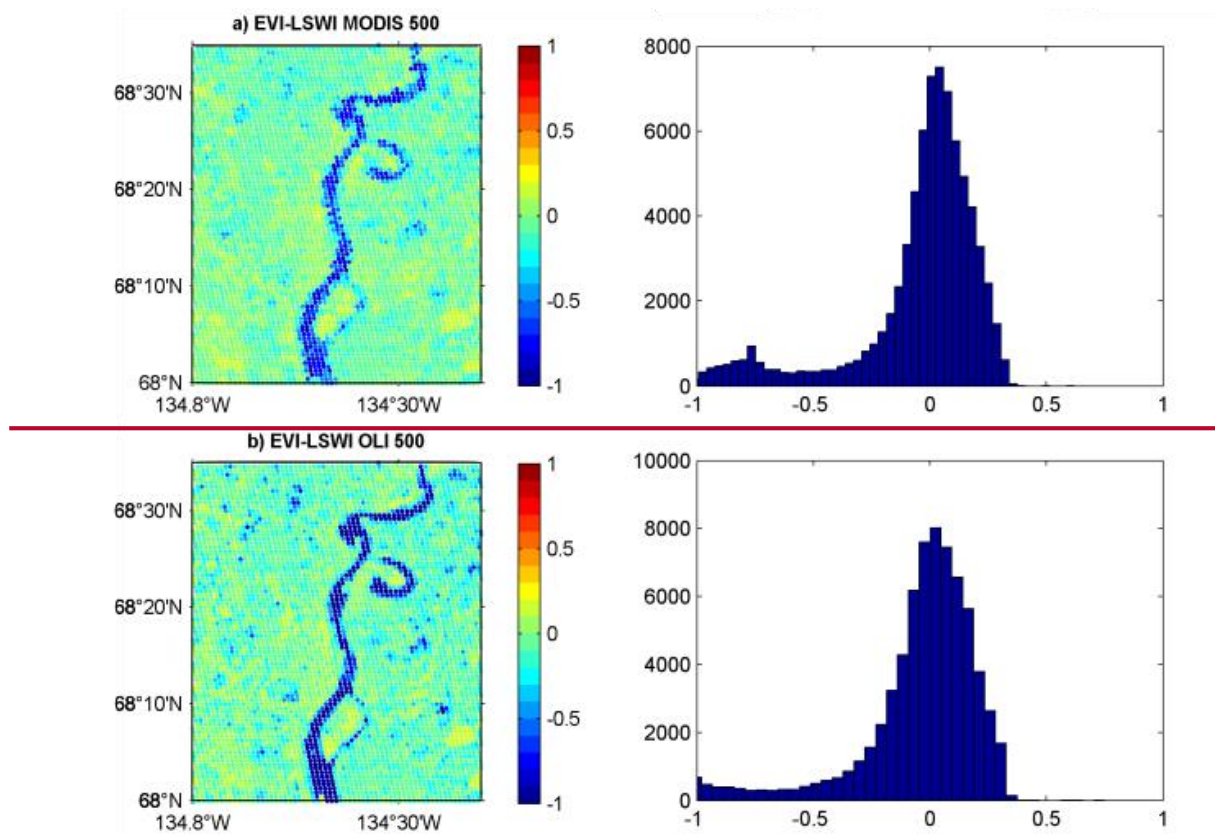


Figure 4: Map of difference between EVI and LSWI indices and associated histogram in July 2013 for (a) MODIS and (b) OLI 500

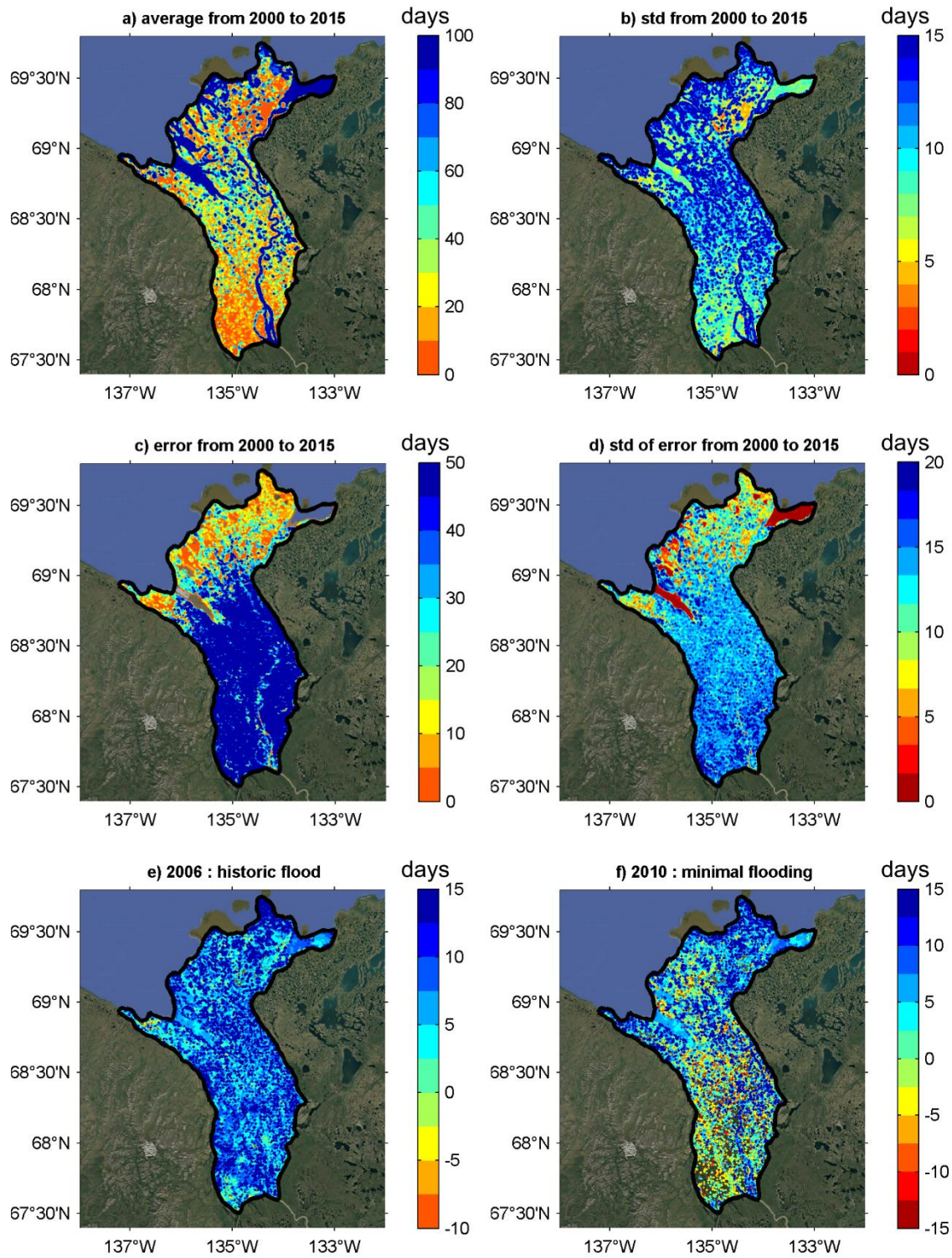


Figure 35: Maps of surface water extent duration for (a) annual average from 2000 to 2015, (b) annual standard deviation from 2000 to 2015, (c) error average from 2000 to 2015, (d) standard deviation of error from 2000 to 2015, difference between annual average land water surface duration from 2000 to 2015 and land water surface duration during (e) 2006 associated with the highest flood event, and (f) 2010 associated with the lowest flood event recorded over the period.

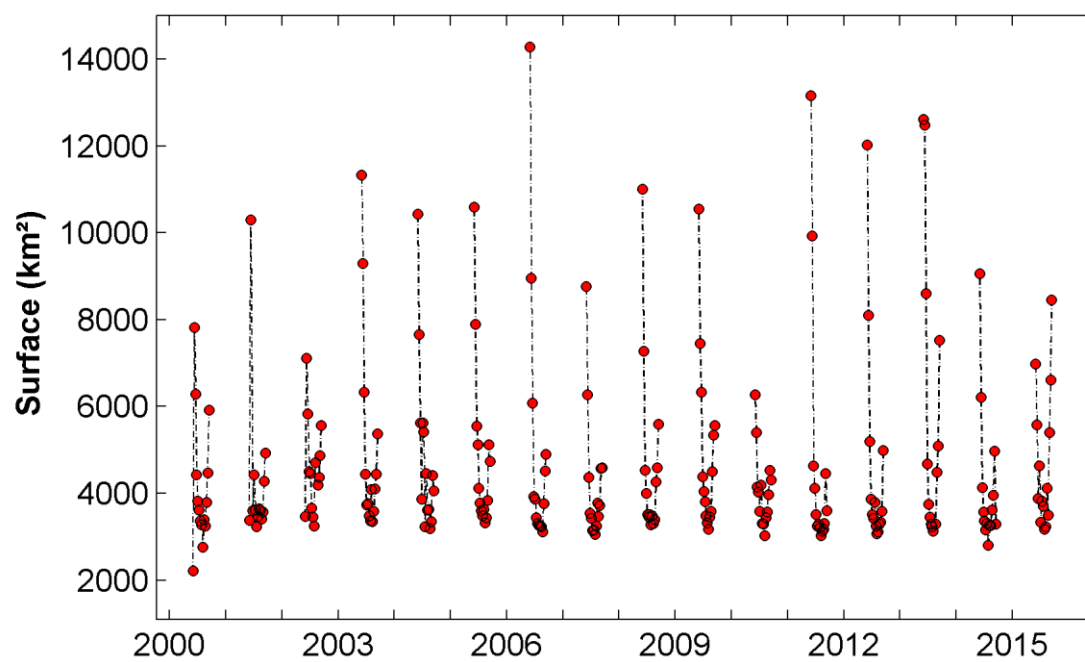


Figure 6: Time series of surface water extent from 2000 to 2015, between June and September, derived from the MODIS images.

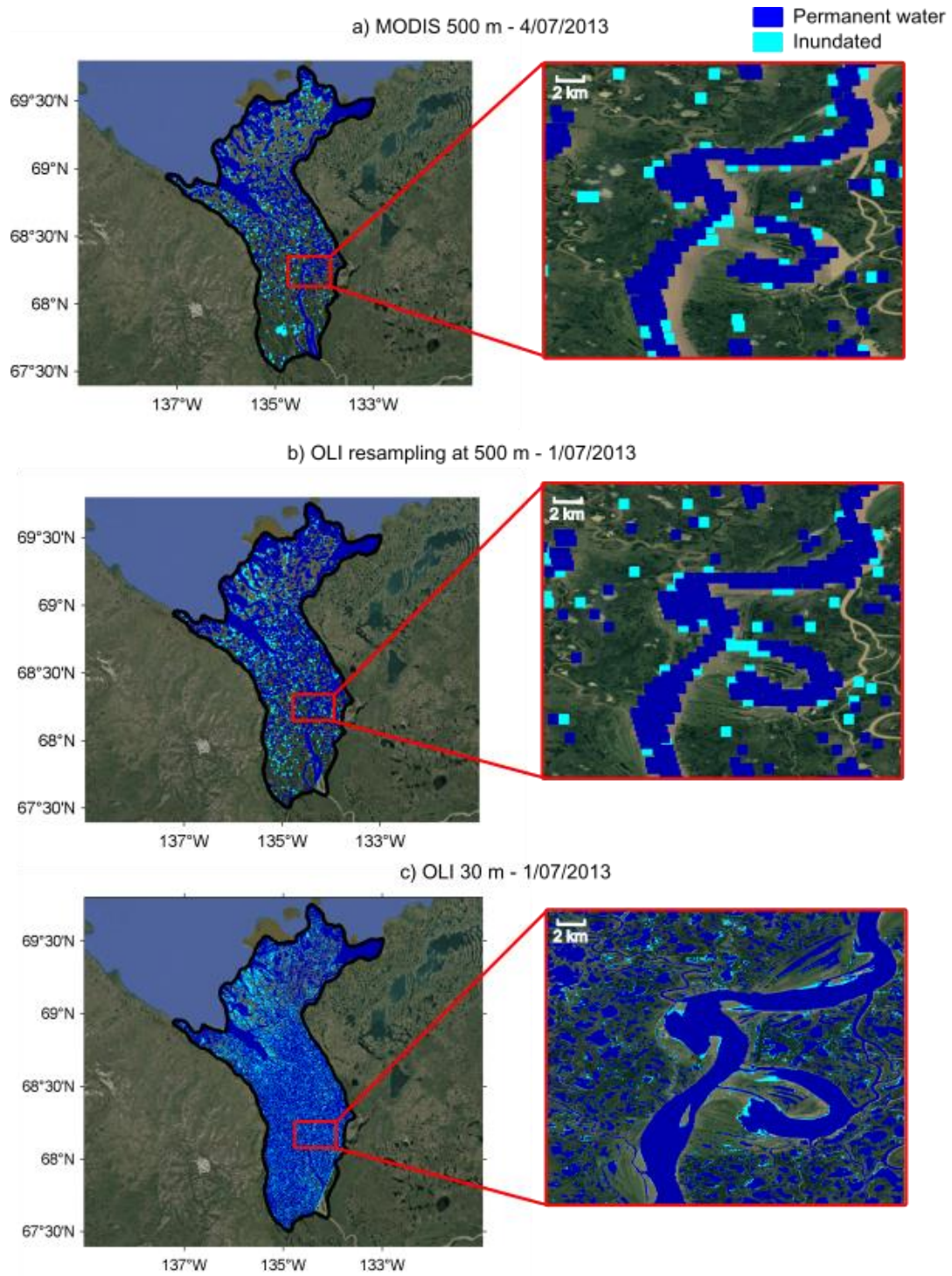


Figure 7: Surface water extent estimated in July 2013 using (a) MODIS at 500 m (b) OLI at 500 m and (c) OLI at 30 m. Permanent water bodies appear in blue and inundated areas in light blue.

Table 1: Validation of surface water extents (km²) determined using OLI 30 m, OLI 500 m, and MODIS 500 m images with Emmerton et al. (2007)

| | MODIS : 04/07/2013 OLI : 01/07/2013 | MODIS : 05/08/2013 OLI : 02/08/2013 |
|---|--|--|
| MODIS 500 m | 3,798 | 3,298 |
| OLI 500 m | 4,499 | 3,859 |
| Emmerton et al., 2007 (channels+wetlands, km ²) | 3,358 | 3,358 |
| Difference between MODIS 500 and Emmerton et al., 2007 | 440 km ² (13 %) | 60 km ² (2 %) |
| Difference between OLI 500 and Emmerton et al., 2007 | 1,141 (34 %) | 500 (15 %) |
| OLI 30 m | 7,685 | 7,156 |
| Emmerton et al., 2007 (channels+lakes+wetlands, km ²) | 6,689 | 6,689 |
| Difference between OLI 30 and Emmerton et al., 2007 | 996 km ² (13 %) | 467 km ² (7 %) |

Table 2: Satellite validation of surface water extent using OLI 30, OLI 500 and MODIS 500 m.

| Date | Permanent water MODIS (km²) | Permanent water OLI 500 (km²) | Permanent water OLI 30 (km²) | Inundated surfaces MODIS (km²) | Inundated surfaces OLI 500 (km²) | Inundated surfaces OLI 30 (km²) |
|--|---|---|--|--|--|---|
| MODIS : 04/07/2013 OLI : 01/07/2013 | 3,167 | 3,809 | 7,058 | 577 | 690 | 627 |
| MODIS : 05/08/2013 OLI : 02/08/2013 | 2,885 | 3,809 | 7,058 | 250 | 50 | 98 |

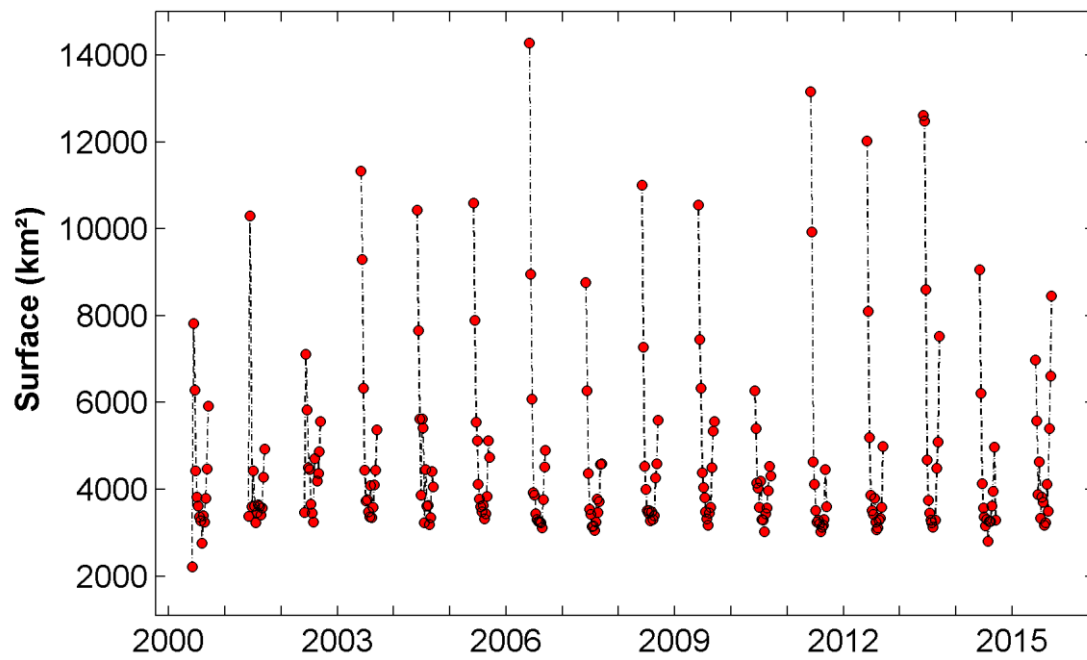


Figure 4: Time series of surface water extent from 2000 to 2015, between June and September, derived from the MODIS images.

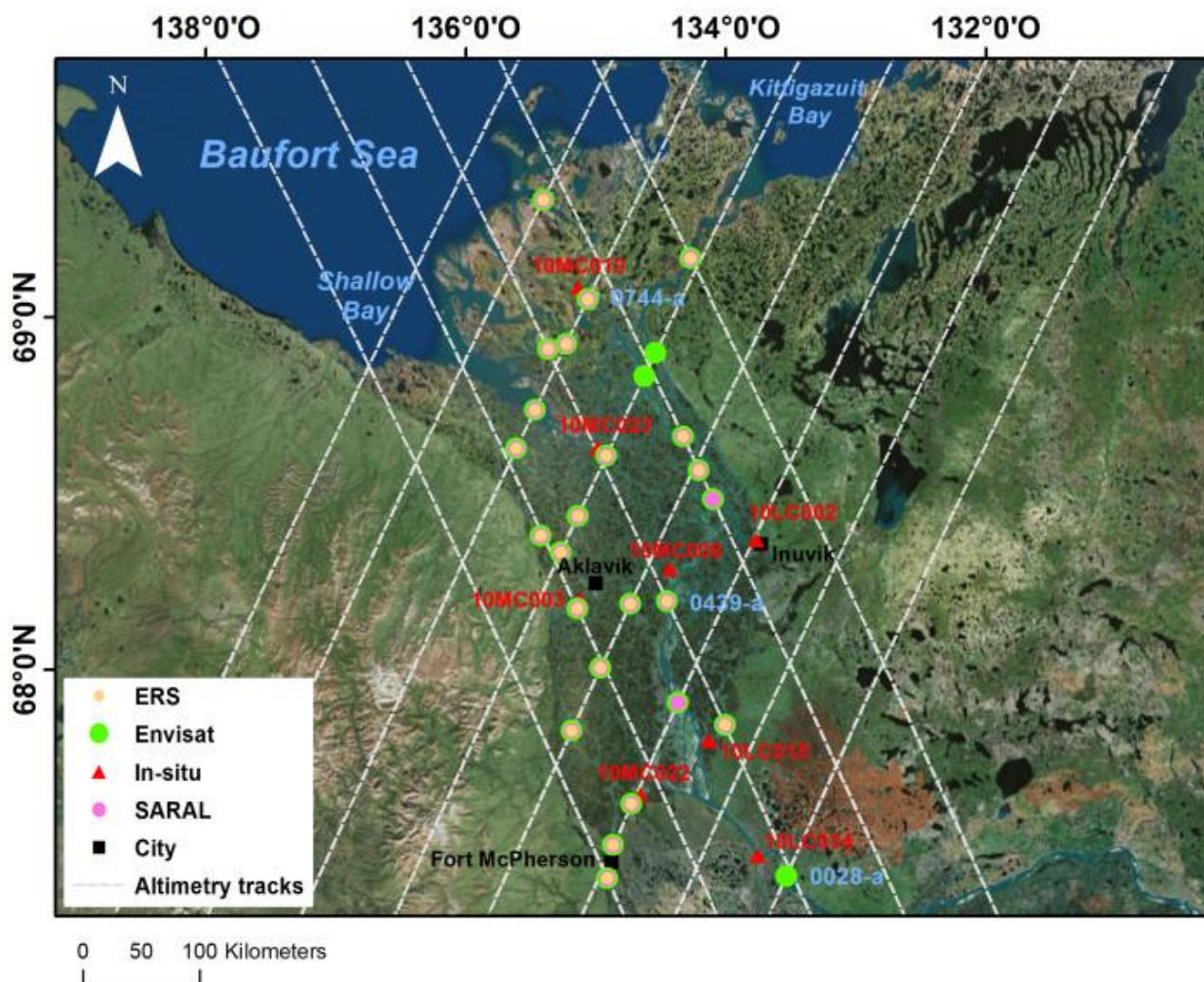


Figure 85: Locations of virtual stations (VS) in the Mackenzie Delta for ERS-2 (yellow dots), Envisat (green dots) and SARAL (purple dots) altimetry missions. Altimetry tracks appear in grey. *In situ* stations are represented using red triangles.

Table 3: Statistic parameters obtained between altimetry-based water levels from altimetry multi-mission and *in situ* water levels

| Virtual station (SV) | In situ station | Altimetry mission | Distance (km) | River width at VS (m) | N | r | RMS (m) | R ² | Bias (m) | Bias ICESat (m) |
|----------------------|-----------------|-------------------|---------------|-----------------------|----|-------|---------|----------------|----------|-----------------|
| 0439-a | 10MC008 | ERS-2 | 11.44 | 1950 | 5 | 0.76 | 0.5 | 0.58 | 0.55 | 1.36 |
| | | ENVISAT | | | 24 | 0.89 | 0.5 | 0.81 | 0.15 | 0.65 |
| | | SARAL | | | 8 | 0.96 | 0.35 | 0.93 | -0.95 | -0.15 |
| 0983-c | 10MC003 | ERS-2 | 3.1 | 360 | 20 | 0.69 | 0.7 | 0.47 | - | - |
| | | ENVISAT | | | 26 | 0.66 | 0.89 | 0.44 | - | - |
| | | SARAL | | | 6 | 0.9 | 0.4 | 0.8 | - | - |
| 0114-c | 10MC022 | ERS-2 | 1.9 | 430 | 14 | -0.38 | 2.82 | 0.14 | - | - |
| | | ENVISAT | | | 23 | 0.8 | 1.17 | 0.64 | - | - |
| | | SARAL | | | 7 | 0.14 | 0.73 | 0.02 | - | - |
| 0200-d | 10MC023 | ERS-2 | 4.11 | 630 | 17 | 0.08 | 4.3 | 0 | - | - |
| | | ENVISAT | | | 22 | 0.87 | 0.33 | 0.75 | - | - |
| | | SARAL | | | 6 | 0.76 | 0.3 | 0.57 | - | - |
| 0744-a | 10MC010 | ERS-2 | 5.16 | 850 | 5 | 0.88 | 0.1 | 0.77 | - | -1.28 |
| | | ENVISAT | | | 24 | 0.93 | 0.15 | 0.87 | - | -1.17 |
| | | SARAL | | | 2 | 0.99 | 0.15 | 0.99 | - | -2.19 |
| 0439-d | 10LC015 | ERS-2 | 7.2 | 380 | 20 | 0.92 | 0.83 | 0.86 | - | - |
| | | ENVISAT | | | 28 | 0.65 | 1.75 | 0.43 | - | - |
| | | SARAL | | | 5 | 0.95 | 1.3 | 0.9 | - | - |
| 0525-a | 10MC002 | ENV | 16.31 | 500 | 29 | 0.77 | 1.45 | 0.6 | - | - |
| 0028-a | 10LC014 | ENV | 16.05 | 1360 | 17 | 0.83 | 1.84 | 0.7 | - | 2.35 |

|

Table 3: Statistic parameters obtained between altimetry-based water levels from ERS-2 and *in situ* water levels

| Virtual station (SV) | In-situ station | Distance (km) | River width at VS (m) | N | r | RMS (m) | R ² | Bias (m) | Bias ICESat (m) |
|-------------------------|-----------------|---------------|-----------------------|----|-------|---------|----------------|----------|-----------------|
| ERS-2-0439-a | 10MC008 | 11.44 | 1950 | 5 | 0.76 | 0.5 | 0.58 | 0.55 | 1.36 |
| ERS-2-0983-e | 10MC003 | 3.1 | 360 | 20 | 0.69 | 0.7 | 0.47 | - | - |
| ERS-2-0114-e | 10MC022 | 1.9 | 430 | 14 | -0.38 | 2.82 | 0.14 | - | - |
| ERS-2-0200-d | 10MC023 | 4.11 | 630 | 17 | 0.08 | 4.3 | 0 | - | - |
| ERS-2-0744-a | 10MC010 | 7.2 | 380 | 5 | 0.88 | 0.1 | 0.77 | - | -1.28 |
| ERS-2-0439-d | 10LC015 | 7.2 | 380 | 20 | 0.92 | 0.83 | 0.86 | - | - |

Table 4: Statistic parameters obtained between altimetry-based water levels from ENVISAT and *in situ* water levels

| Virtual station (SV) | In-situ station | Distance (km) | River width at VS (m) | N | r | RMS (m) | R ² | Bias (m) | Bias ICES at (m) |
|----------------------|-----------------|---------------|-----------------------|----|------|---------|----------------|----------|------------------|
| ENV-0439-a | 10MC008 | 11.44 | 1950 | 24 | 0.89 | 0.5 | 0.81 | 0.15 | 0.65 |
| ENV-0983-e | 10MC003 | 3.1 | 360 | 26 | 0.66 | 0.89 | 0.44 | - | - |
| ENV-0114-e | 10MC022 | 1.9 | 430 | 23 | 0.8 | 1.17 | 0.64 | - | - |
| ENV-0200-d | 10MC023 | 4.11 | 630 | 22 | 0.87 | 0.33 | 0.75 | - | - |
| ENV-0525-a | 10MC002 | 16.31 | 500 | 29 | 0.77 | 1.45 | 0.6 | - | - |
| ENV-0744-a | 10MC010 | 5.16 | 850 | 24 | 0.93 | 0.15 | 0.87 | - | -1.17 |
| ENV-0028-a | 10LC014 | 16.05 | 1360 | 17 | 0.83 | 1.84 | 0.7 | - | 2.35 |
| ENV-0439-d | 10LC015 | 7.2 | 380 | 28 | 0.65 | 1.75 | 0.43 | - | - |

Table 5: Statistics parameters obtained between altimetry-based water levels from SARAL and *in situ* water levels

| Virtual station (SV) | In-situ station | Distance (km) | River width at VS (m) | N | r | RMS (m) | R ² | Bias (m) | Bias ICESat (m) |
|----------------------|-----------------|---------------|-----------------------|---|------|---------|----------------|----------|-----------------|
| SARAL-0439-a | 10MC008 | 11.44 | 1950 | 8 | 0.96 | 0.35 | 0.93 | -0.95 | -0.15 |
| SARAL-0983-e | 10MC003 | 3.1 | 360 | 6 | 0.9 | 0.4 | 0.8 | - | - |
| SARAL-0114-e | 10MC022 | 1.9 | 430 | 7 | 0.14 | 0.73 | 0.02 | - | - |
| SARAL-0200-d | 10MC023 | 4.11 | 630 | 6 | 0.76 | 0.3 | 0.57 | - | - |
| SARAL-0744-a | 10MC010 | 5.16 | 850 | 2 | 0.99 | 0.15 | 0.99 | - | -2.19 |
| SARAL-0439-d | 10LC015 | 7.2 | 380 | 5 | 0.95 | 1.3 | 0.9 | - | - |

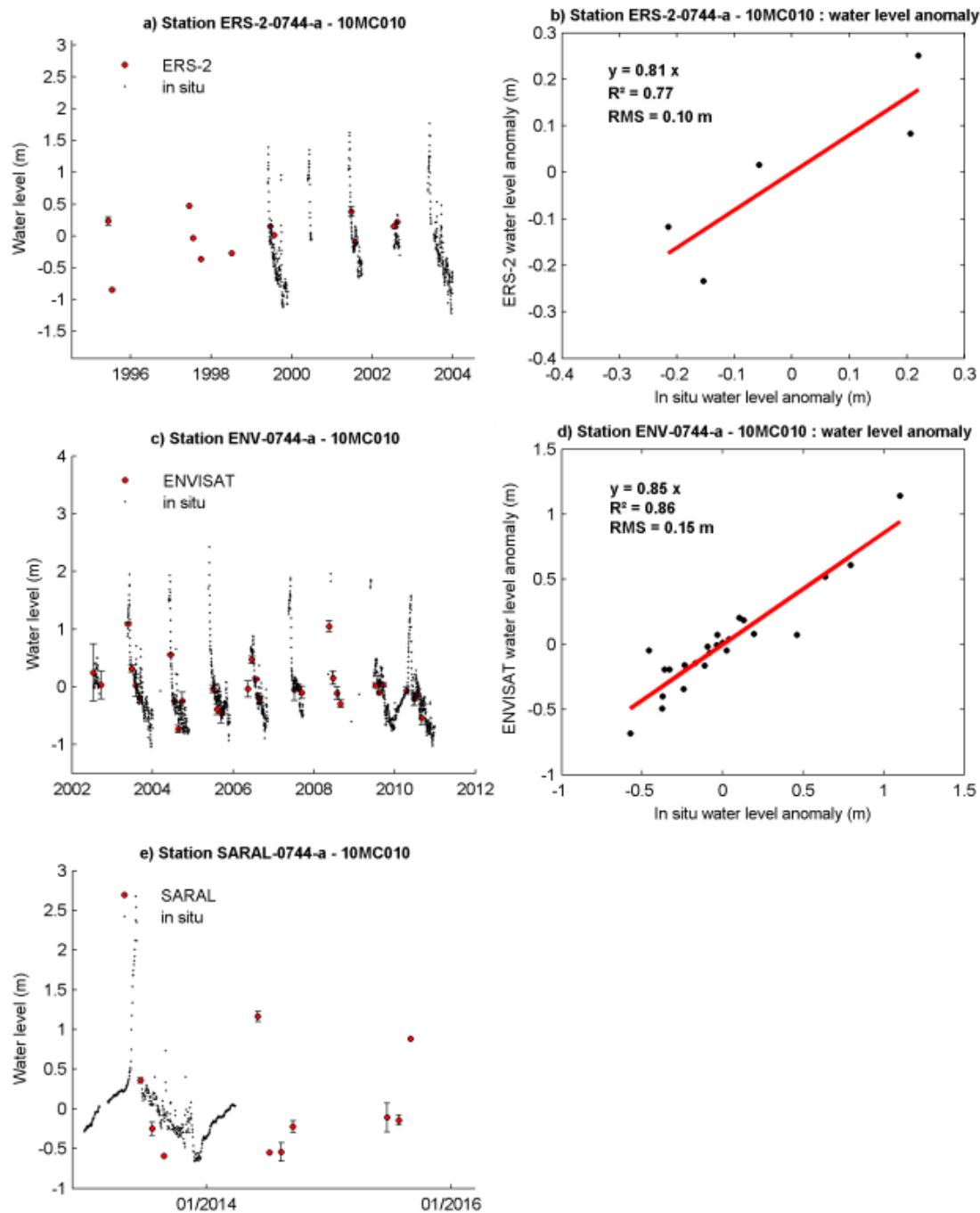


Figure 96: Altimetry-based water levels from 1995 to 2015 compared with in situ water levels for the station 0744-a located in the downstream part in the Mackenzie Delta (a) using ERS-2 mission and (b) water level anomaly with statistic parameters, (c) using ENVISAT mission and (d) water level anomaly with statistic parameters and (e) using SARAL mission

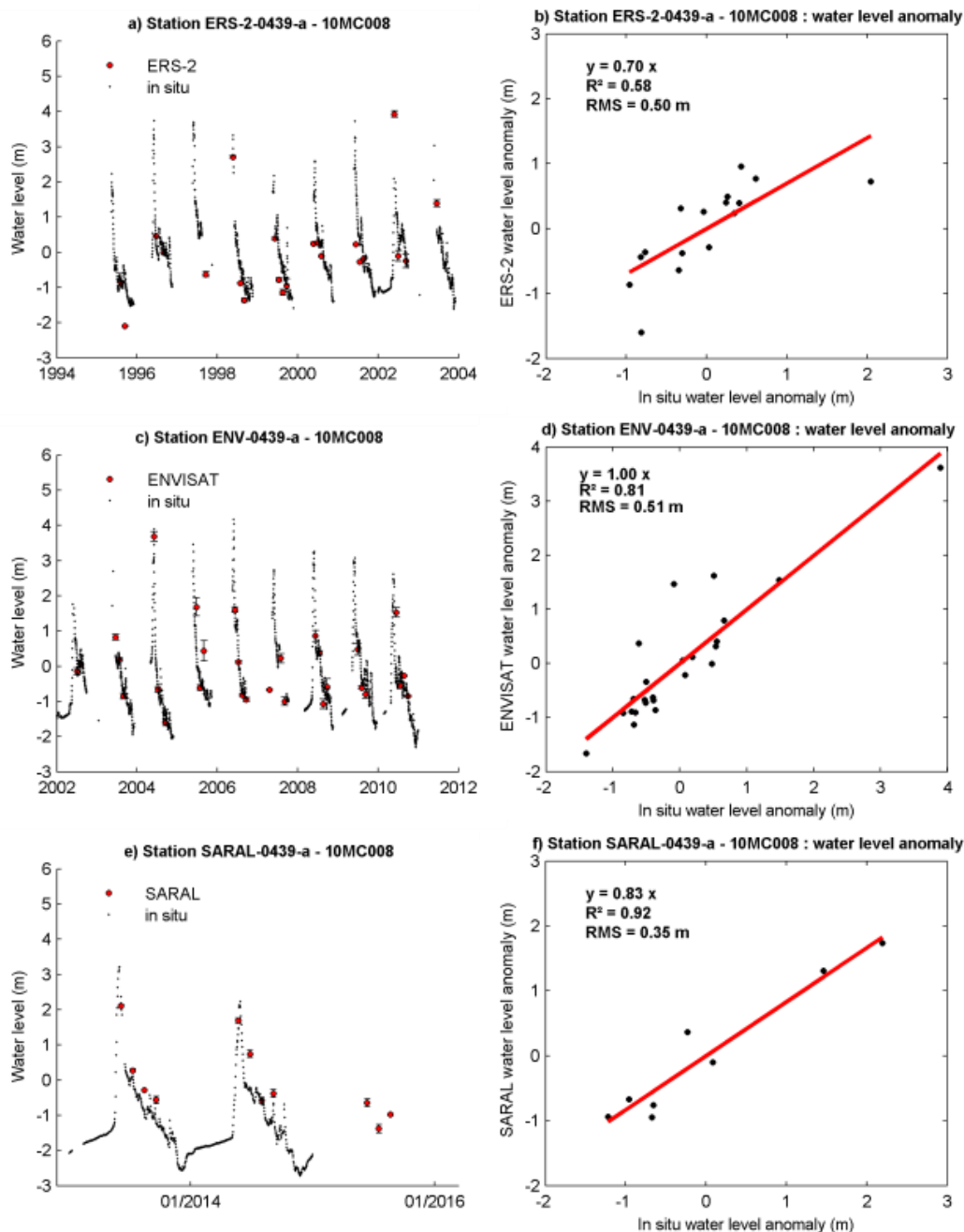


Figure 740: Altimetry-based water levels from 1995 to 2015 compared with in situ water levels for the station 0439-a located in the center in the Mackenzie Delta (a) using ERS-2 mission and (b) water level anomaly with statistic parameters, (c) using ENVISAT mission and (d) water level anomaly with statistic parameters, (e) using SARAL mission and (f) water level anomaly with statistic parameters

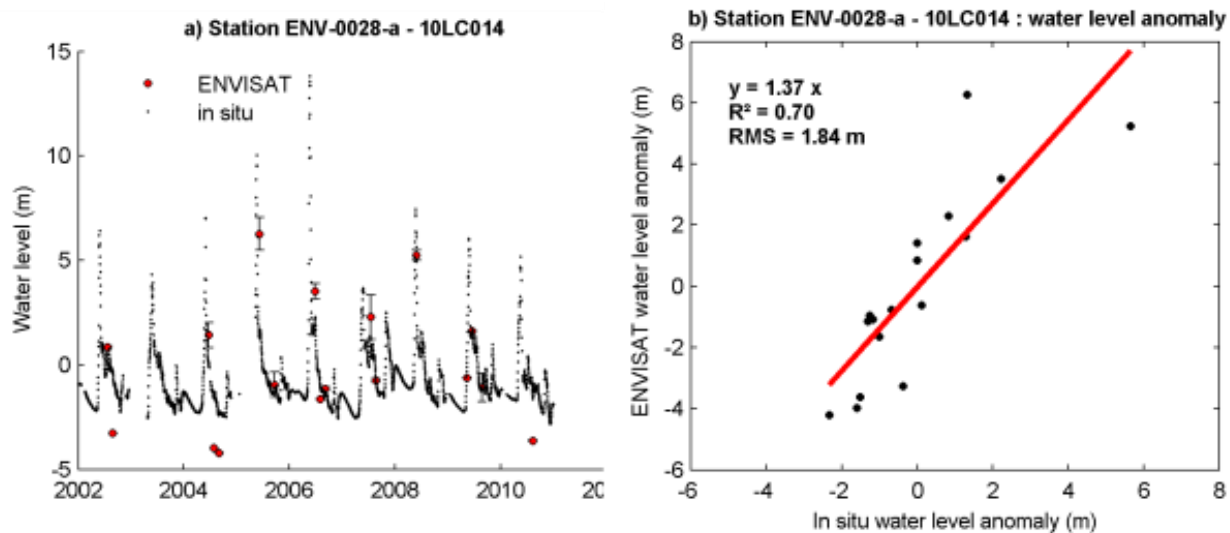
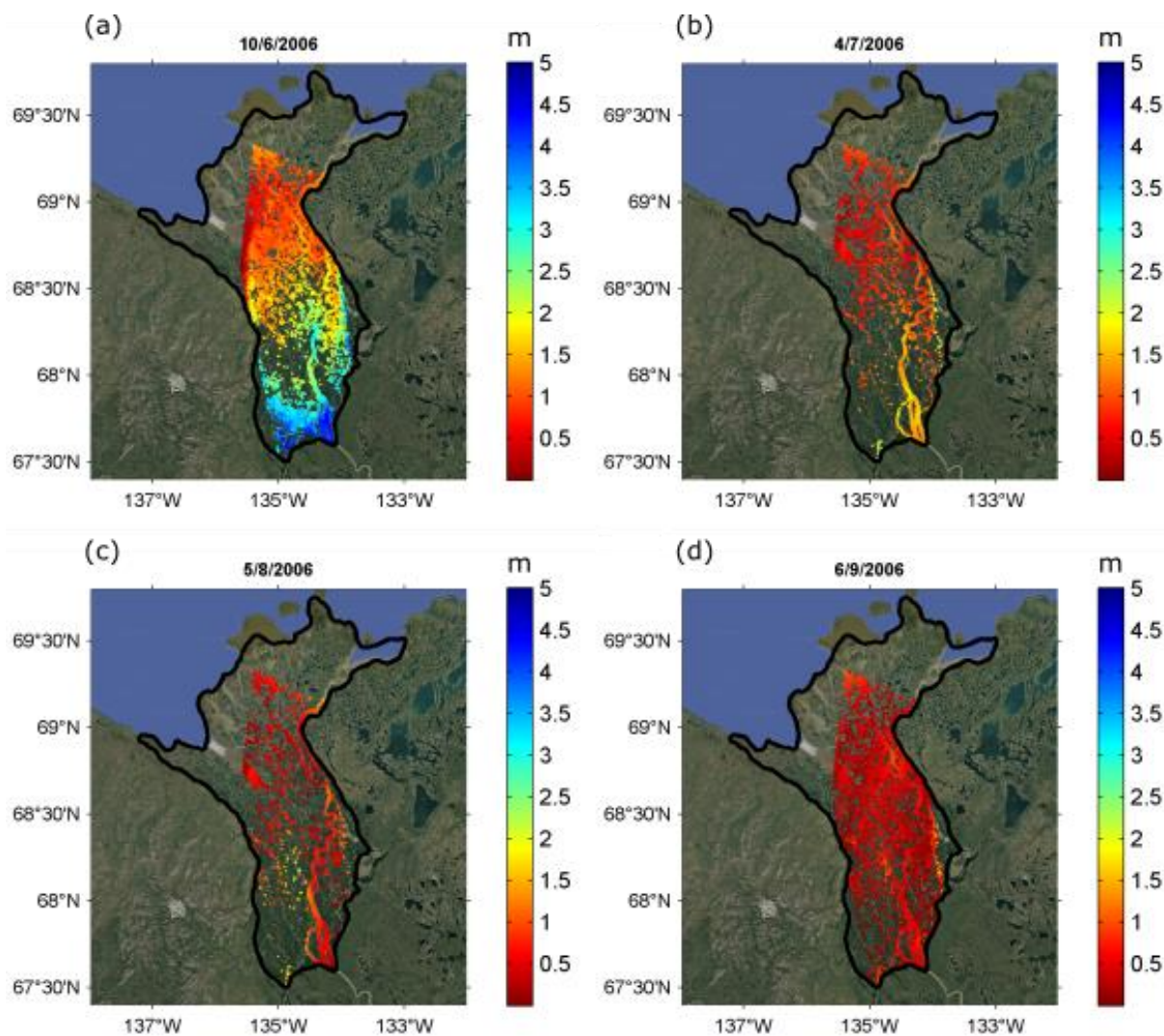


Figure 844: Altimetry-based water levels from 2002 to 2010 compared to in situ water levels for the station 0439-a located in the center in the Mackenzie Delta (a) using ENVISAT mission and (b) water level anomaly with statistic parameters



5 **Figure 9.912:** Water level maps in the Mackenzie Delta in 2006 (historic flood) obtained combining inundated surfaces determined using MODIS images with altimetry-derived water levels (a) in June, (b) in July, (c) in August and (d) in September

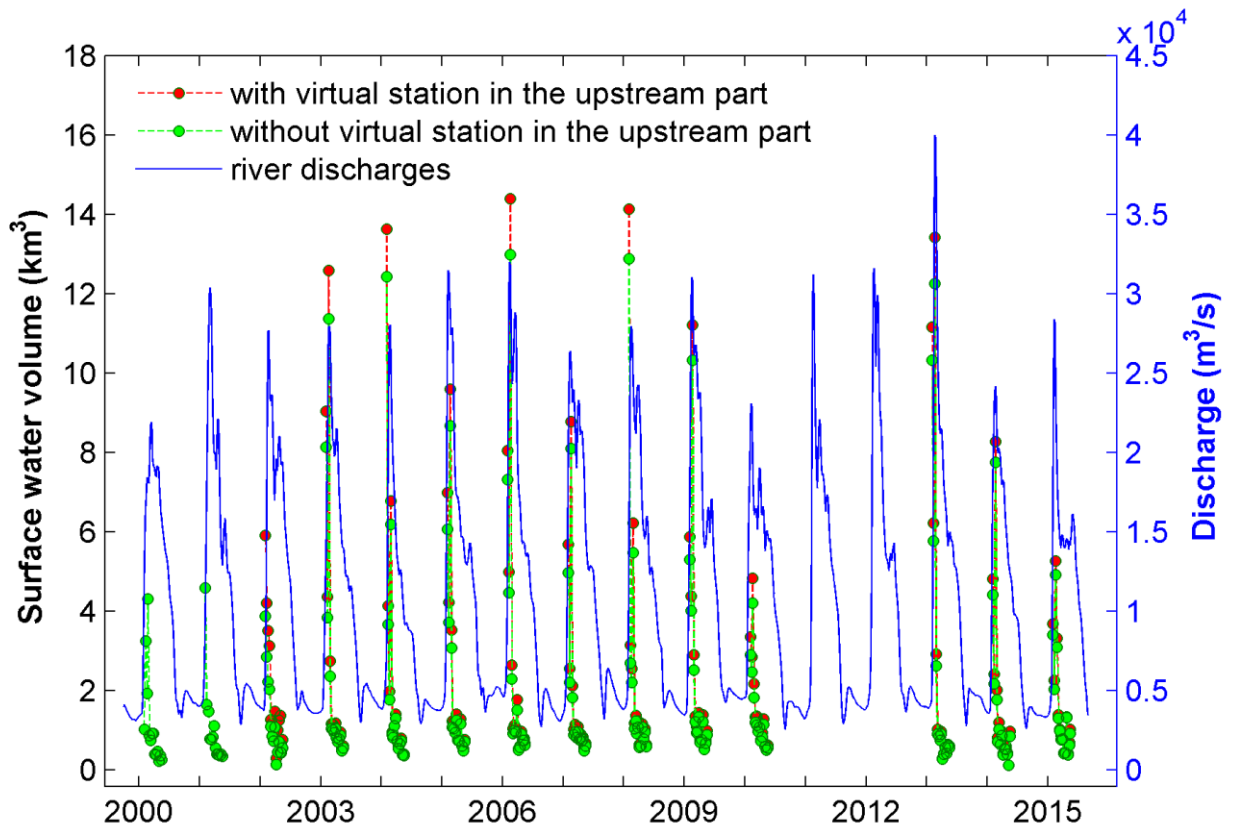


Figure 1010-13: Surface water volume from 2000 to 2015, determined by combining inundated surfaces from MODIS with altimetry data. 167 red points correspond to surface water volume obtained with a virtual station located in the upstream part of the Delta, green points to surface water volume without a virtual station located in the upstream part of the Delta. The Mackenzie River Delta discharges at 10LC014 gauge station appear in blue.

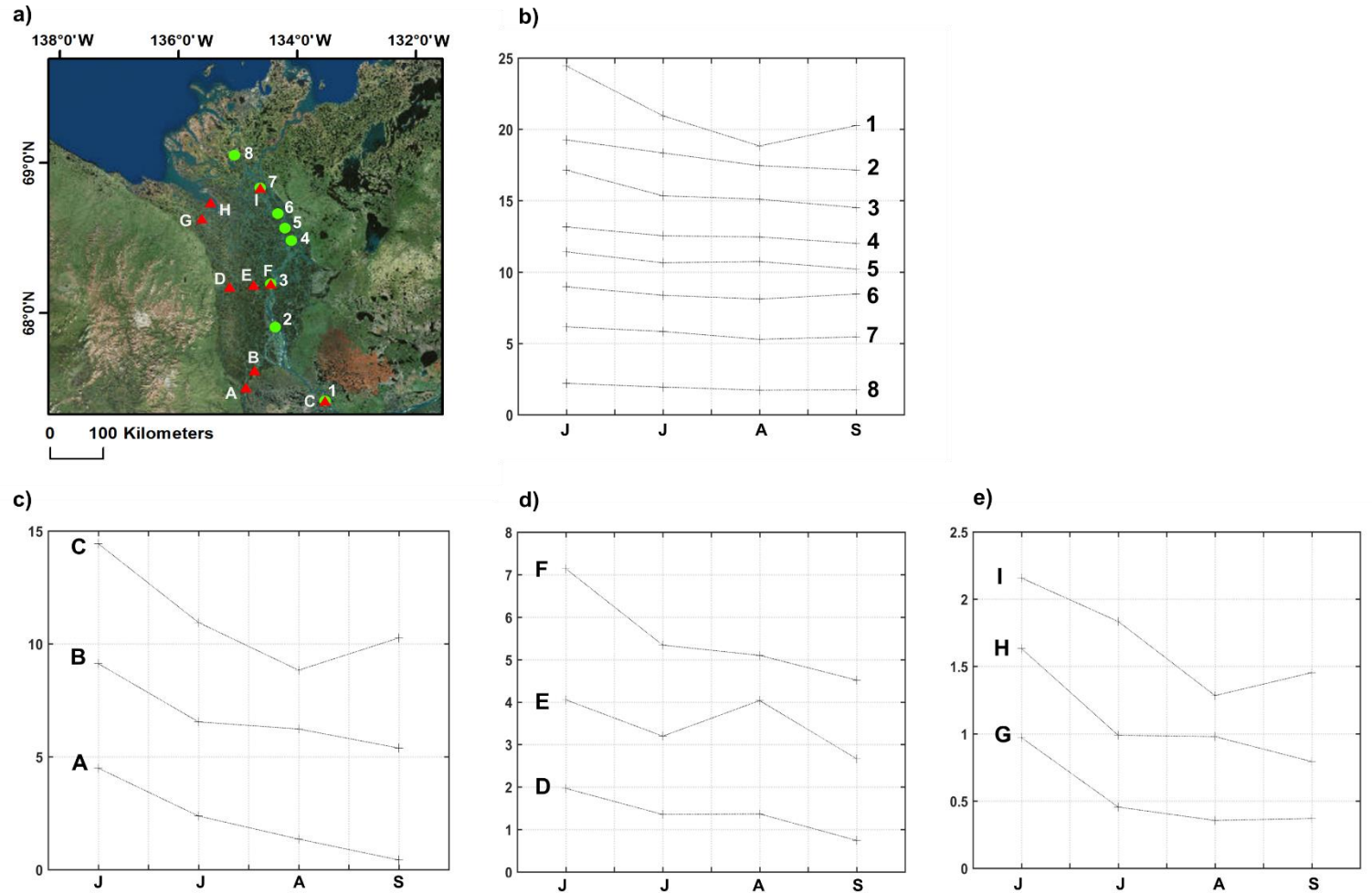


Figure 11: Temporal and spatial variations of surface water levels in the Mackenzie Delta a) Location of virtual stations used to analyse spatial variations, green dots are corresponding to latitudinal variations along the Mackenzie River (from number 1 to 8) and red triangles are corresponding to longitudinal variations at 3 different latitudes (letters from A to I), b) surface water levels time-series along the Mackenzie River at different latitudes, c), d) and e) show surface water levels time series at 3 different latitudes with 3 virtual stations at each latitude to analyse longitudinal spatial variations.

